

TISSUE EQUIVALENT PHANTOMS FOR EVALUATING IN-PLANE TUBE CURRENT
MODULATED CT DOSE AND IMAGE QUALITY

By

RYAN F. FISHER

A THESIS PRESENTED TO THE GRADUATE SCHOOL
OF THE UNIVERSITY OF FLORIDA IN PARTIAL FULFILLMENT
OF THE REQUIREMENTS FOR THE DEGREE OF
MASTER OF SCIENCE

UNIVERSITY OF FLORIDA

2006

Copyright 2006

by

Ryan F. Fisher

ACKNOWLEDGMENTS

I thank my supervisory committee chair (Dr. David E. Hintenlang) for his guidance, help, and patience throughout the course of this research. I also thank Dr. Manuel Arreola for his expertise and direction in the clinical aspects of the research.

TABLE OF CONTENTS

	<u>page</u>
ACKNOWLEDGMENTS	3
LIST OF TABLES	6
LIST OF FIGURES	7
ABSTRACT.....	9
CHAPTER	
1 INTRODUCTION AND BACKGROUND	11
Introduction.....	11
Basic Principles of Tube Current Modulation	12
Angular Modulation	13
Z-Axis Modulation	14
Simulation and Phantom Studies with Tube Current Modulation.....	15
Clinical Studies in Tube Current Modulation	17
Current State of the Art	21
Conclusions	23
Purpose of Study.....	24
Overview	25
Approach	25
2 TISSUE EQUIVALENT MATERIAL DEVELOPMENT	36
Silicone-Based Rubber Material Testing.....	36
Sample Preparation.....	37
Sample Testing	37
Urethane-Based Rubber Material Testing	38
Material Testing.....	39
Results of Attenuation and Density Testing.....	40
Materials Testing with PMC 121/30.....	41
Further Testing	42
3 ELLIPTICAL PHANTOM CONSTRUCTION	51
Materials and Methods	51
Improved Construction Methods	52

4	PHANTOM TESTING	57
	Materials and Methods	57
	Phantom Dose Measurement	57
	Phantom Image Quality Measurement	59
	Comparison of Modulated and Fixed Tube Current Techniques	60
	Results and Discussion	60
	Image Uniformity Measurements	60
	Dose Measurements	62
	Overall Trends	63
	Comparison of Modulated and Fixed Tube Current Techniques	63
	Conclusions	65
5	FUTURE WORK	72
	APPENDIX	74
	LIST OF REFERENCES	77
	BIOGRAPHICAL SKETCH	78

LIST OF TABLES

<u>Table</u>		<u>page</u>
1-1	Results of phantom dose reduction studies.....	33
1-2	Comparison of image noise and diagnostic acceptability.....	34
1-3	Reductions in tube current time product with Z-axis modulation	34
2-1	Ecoflex samples prepared with various additives.....	44
2-2	Material properties of various Smooth-On rubbers	45
2-3	List of slabs poured with 121/30 as a base	49

LIST OF FIGURES

<u>Figure</u>	<u>page</u>
1-1 Phantom demonstration of angular tube current modulation.....	28
1-2 Real-time tube current modulation.	28
1-3 Z-axis modulation.	29
1-4 Z-axis modulation.	30
1-5 Summary of phantoms and associated path-lengths	31
1-6 Image noise as a function of modulation parameter.	32
1-7 Kidney phantom.....	35
2-1 Three tissue equivalent slabs curing in epoxy molds.....	44
2-2 Relative attenuation of samples.	44
2-3 Relative attenuation of Ecoflex™ based tissue equivalent materials	45
2-4 Slabs of PMC 780, 744, 121/30 and 121/50 urethane-based rubbers.....	46
2-5 Experimental setup for attenuation measurement.....	46
2-6 Full experimental setup.....	47
2-7 Comparison of attenuation coefficients of urethane based rubbers.....	47
2-8 Comparison of densities of urethane based rubbers.	48
2-9 Attenuation coefficients of PMC 121/30 based materials.	48
2-10 Densities of PMC 121/30 based materials	49
2-11 Attenuation values of 121/30 with various additives.....	50
3-1 Diagram of proposed phantom design.	54
3-2 Elliptical phantom mold.....	54
3-3 CTDI head phantom centered in phantom mold.....	55
3-4 Phantom mold filled with urethane liquid rubber.	55
3-5 Five elliptical tissue equivalent phantoms of increasing major axis.....	56

4-1	Experimental setup for dose measurements.....	66
4-2	Screen capture of a CT scan of an elliptical phantom surrounding a uniform region of an image quality phantom.....	67
4-3	CT number uniformity as a function of phantom major axis and reference mAs setting.....	68
4-4	Percent increase in CT number uniformity for increasing reference mAs settings	68
4-5	Percent increase in CT uniformity with error bars for 190 reference mAs setting.....	69
4-6	Increases in dose as a result of changes in phantom major axis length and reference mAs setting.	69
4-7	Comparison of image quality between modulated and fixed tube current techniques.	70
4-8	Comparison of dose between modulated and fixed tube current techniques.....	71
A-1	CT number uniformity as a function of phantom major axis.....	74

Abstract of Thesis Presented to the Graduate School
of the University of Florida in Partial Fulfillment of the
Requirements for the Degree of Master of Science

TISSUE EQUIVALENT PHANTOMS FOR EVALUATING IN-PLANE TUBE CURRENT
MODULATED CT DOSE AND IMAGE QUALITY

By

Ryan F. Fisher

December 2006

Chair: David Hintenlang
Major: Nuclear Engineering Sciences

A compressible, flexible, urethane-based tissue equivalent material was developed and utilized in the production of five ellipsoid-shaped phantoms for evaluating the in-plane tube current modulation performance of multi-slice CT scanners. The created phantoms were designed to be integrated with a computed tomography dose index (CTDI) dose assessment head phantom. Each phantom has a minor axis of 16 cm (corresponding to the diameter of the CTDI head phantom), with major axes ranging from 26 to 36 cm. A Siemens Somatom Sensation 16 CT scanner (Malvern, PA) was used to take central axis ion chamber dose measurements of each phantom using six different reference mAs settings with Siemens CARE Dose4D™ tube current modulation system. Image uniformity from each scan was measured as a method of tracking changes in image quality as a result of changes in the reference mAs setting. Tests were also performed comparing dose and image quality for scans using modulated and fixed tube current techniques.

Image uniformity was found to be relatively constant for each reference mAs setting regardless of phantom major axis length, proving the proper functionality of the in-plane component of the CARE Dose4D™ system. Image uniformity was found to increase as the reference mAs setting was increased, at the expense of higher doses. In comparing modulated

versus fixed tube current techniques, dose savings of up to 63% were observed, but at the expense of slightly noisier images.

Elliptical phantoms of varying major axis length can be easily and effectively used to test the performance of in-plane tube current modulation systems in multi-slice CT scanners. Such phantoms can also prove useful in comparing image quality and dose measurements between differing commercial CT scanners.

CHAPTER 1 INTRODUCTION AND BACKGROUND

Introduction

X-ray Computed Tomography exams have become increasingly popular because of recent technological developments (such as multi detector spiral CT and greatly reduced scan times that allow a large amount of diagnostic information to be collected in a short period of time). As volumetric CT becomes more commonplace, concerns have arisen over increases in patient dose as a result of wider beams and more frequent exams. Studies have shown that although CT accounts for only 11% of x-ray based examinations in the United States, it delivers over 65% of the total radiation dose associated with medical imaging.¹ Effective doses for standard protocols of neck, chest abdomen and lumbar spine examinations can range from 3-15 mSv in adults, and currently there are no limits in place on the amount of radiation delivered per scan in the US.² Radiation exposure from CT is of particular concern for pediatric studies due to children's relative increased lifetime cancer risk and higher radiosensitivity compared to adults.² It should be noted that despite these statistics and facts, CT remains a low dose imaging modality. However, in the interest of keeping radiation exposure as low as reasonably achievable, methods to reduce CT dose and improve image quality have been explored.

Numerous solutions have been suggested in response to dose concerns, including a general lowering of tube current techniques for all exams.² Although this suggestion would reduce patient doses, such a reduction would come at the expense of noisier images, given that image noise is related to the number of photons incident on the detector.³ A decrease in tube current could thus compromise image resolution and low contrast detectability in medical images, possibly leading to misdiagnosis.³ As an alternate approach, CT scanner manufacturers have developed technologies for lowering patient doses without sacrificing image quality. These

technologies are referred to as tube current modulation, and act to adjust the x-ray tube output during the CT scan in either the x-y plane (angular modulation) or in the Z direction (Z-axis modulation) in response to changes in patient anatomy and attenuation in order to reduce dose and maintain a constant image quality throughout the scan.³

Basic Principles of Tube Current Modulation

In Computed Tomography exams, selectable techniques such as tube current and tube potential determine the photon fluence output of the x-ray tube.¹ This fluence, along with the attenuation characteristics of the patient, determines patient dose as well as the number of photons reaching the detectors, which in turn determines reconstructed image noise characteristics.¹⁻³ If all other variables are held constant, a reduction in tube current leads to a reduction in patient dose, but an increase in quantum noise or mottle in the reconstructed image. Images with too much quantum noise may obscure low contrast lesions or tumors that would normally be visible in less noisy images.¹⁻³

In conventional CT, a technologist selects the tube current and tube potential based on patient characteristics such as size and weight, as well as based on the particular exam being performed. These techniques are held constant for each slice throughout the exam. Since patients are not homogeneous in composition, nor circular in exterior body shape, these fixed techniques lead to variable attenuation though the body and as such, a variable number of photons reaching the detectors on the opposite side of the patient for different projection angles.⁴ Certain anatomical areas, such as the shoulders, are problematic in that lateral views have much higher attenuation, up to three orders of magnitude higher,⁴ than anteroposterior views of the same area. In these instances, tube current must be increased to allow more photons to reach the detector in order to minimize reconstruction artifacts due to high image noise in those planes.

The result of this increase in tube current is an increased patient dose throughout the entire scan area of the exam if the techniques are held constant for the entire exam area.⁴

In response to these problems, CT manufacturers have developed automatic tube current modulation techniques that allow the tube current to be automatically adjusted during a CT examination in order to provide lower patient doses and constant image noise characteristics. Tube current in low attenuation projections can be greatly reduced without loss of image quality, thus reducing patient dose for the exam. There are currently two major strategies employed by manufacturers to accomplish this task; angular and Z-axis modulation.¹

Angular Modulation

Angular modulation was first developed by GE Medical Systems and works to modulate tube current in the x-y plane within a single rotation of the tube.³ Photon fluence is increased in areas of higher attenuation, such as lateral views through the shoulders, and decreased in areas with lower attenuation, such as AP views through the chest. The first angular modulation system from GE appeared in 1994 (SmartScan), and used two localizer radiographic images, AP and lateral, to determine attenuation values of the patient.³ The tube current was then modulated in a preprogrammed sinusoidal pattern that matched the attenuation characteristics. These systems attained a dose reduction of up to 20% while maintaining a relatively constant level of image noise.³ More recent offerings of the technology by Siemens employ an online real-time anatomy-adapted system (CARE Dose) that automatically adjusts the tube current for a given projection based on the attenuation calculated from the previous rotation.⁵ Thus, tube current is modulated ‘on the fly’ without the need for localizer radiographic images, and is adjusted by attenuation information provided from the previous 180 degree projection as seen in [Figures 1-1](#) and [1-2](#). The CARE Dose system has been shown to produce dose reductions of up to 90% for the anteroposterior projection in regions such as the shoulders with marked asymmetry.³

Philips Medical Systems also uses an angular tube current modulation system (Dose-Right Dose Modulation) in their CT scanners. The Philips technology modulates current within a single tube rotation according to the square root of the attenuation measured during the previous rotation. This modulation technique is based on the fact that image noise is inversely related to the square root of the number of photons captured.³

Z-Axis Modulation

The second major type of tube current modulation technique is Z-axis modulation. This technology also acts to adjust the photon output of the x-ray tube according to patient specific attenuation characteristics, but unlike angular modulation, it does not alter tube current within a single rotation of the x-ray source. Instead, a scout radiographic image is taken of the patient, and the system calculates the photon flux required in each slice in order to maintain a user designated noise level in the reconstructed image.³ The tube current remains constant for each rotation around the patient, but is altered along the length of the patient as the table translates through the beam. Lower current values are thus used in lower attenuation regions, such as the chest, lowering patient dose in comparison to higher attenuation regions such as the pelvis (Figures 1-3 and 1-4).

The user can choose between several noise index values depending on the quality of images required by the exam. The noise index value is approximately equal to the standard deviation of pixel values in the central region of an image of a uniform phantom.³ A higher noise index corresponds to a greater standard deviation of pixel values for similar tissues in an image, but also to a lower overall tube current during the exam and thus lower patient doses. It should be noted that the noise index chosen will not always exactly match the noise in a reconstructed patient image since reconstruction parameters also influence image noise.³ Z-axis modulation is

currently offered by GE medical systems (AutomA) as well as Toshiba and Siemens medical systems, and acts to keep image noise the same in each slice image in an exam.³

Simulation and Phantom Studies with Tube Current Modulation

A two-part study was conducted in 1999 by Michael Gies et al. at the University of Erlangen-Nuremberg in Germany⁴ that tested the theory of tube current modulation with both mathematical simulations as well as phantom studies. In the first part of the study, computational simulations of CT imaging were run on a series of four geometric phantoms including: an elliptical, water-filled, 'shoulder phantom,' an oval shaped, acrylic, 'hip phantom,' an oval, water-filled, 'abdominal phantom,' and a standard water-filled circular phantom (Figure 1-5).

Mathematical simulations were run on all phantoms for a range of modulation factors ranging from 0, corresponding to no modulation (fixed tube current cases), to 1, corresponding to modulation proportional to attenuation. For these varying parameters, image noise in the central pixel of each phantom was computed mathematically to quantify the possible noise reduction and efficiency of tube current modulation.⁴ The effect of tube current modulation was also evaluated on noise in reconstructed images. For all simulations, both a sinusoidal and an attenuation based modulation function were used.

The results of the mathematical simulations showed that a sinusoidal modulation function provides much less noise reduction than attenuation-based methods for all noncircular shaped objects.⁴ It was also shown that image noise is minimized when an attenuation based modulation factor of 0.5 is used, corresponding to current control proportional to the square root of object attenuation. In reconstructed images without tube current modulation, anisotropic noise patterns were visible in the direction of highest attenuation in the object (along the major axis of the ellipse).⁴ As previously mentioned, when modulation is performed according to the square root

of attenuation, image noise is minimized; however, the anisotropic noise structure is still visible in the image. If tube current control is increased to being directly proportional to attenuation, image noise levels rise slightly, but become similar for all projection angles and thus isotropic in the reconstructed image (Figure 1-6). According to the study, a homogeneous, isotropic noise pattern is generally considered superior both aesthetically and diagnostically for CT images, pointing to the fact that absolute lower noise levels may not be optimal for image reconstruction.⁴

The mathematical phantom simulations also showed the dependency of image standard deviation on the inverse square root of photons registered by the detector. For smaller numbers of registered photons, the function changes rapidly, but does not appreciably change for larger numbers of photons. Therefore reducing the number of photons in low attenuation regions will have a minimal impact of image noise, thus allowing for lower patient doses.⁴ Overall the simulation studies confirmed the theory that tube current modulation has the potential to lower patient doses while maintaining or improving image noise characteristics in CT imaging.⁴

In the second part of the German study, actual phantoms with the same dimensions as those utilized in mathematical simulations were used on a Siemens four-slice scanner.⁶ The scanner was equipped with an early prototype of the CAREdose angular modulation system, in which online tube current is modulated based on the previous 180 degree scan of patient attenuation. Tests were also performed with ion chambers in the phantoms to determine the extent of correlation between mAs reduction and actual dose reduction. Utilizing the hip phantom and mathematical simulations, a predicted mAs, and thus dose reduction, of 39.4% was calculated.⁶ This value was similar to the actual measured dose reduction (measured in mGy) in the center of the phantom of 45.1%, proving that actual CT dose reductions are possibly even

larger than would be predicted based solely on mAs reduction.⁶ Since most radiosensitive organs are located in a more or less central position in the body's cross-section, it was determined that the reduction of mAs in studies is a valid and conservative estimate of organ effective dose reduction.⁶

In general, the phantom measurements corresponded to within 10% of the previous mathematical simulations regarding dose reduction and image noise (Table 1-1). Dose reductions of up to 56% were found in highly asymmetrical phantoms such as the shoulder phantom, while maintaining fairly constant image noise. Conversely, in tests where dose remained constant, scans utilizing tube current modulation showed a reduction in image noise compared to scans with constant tube current.⁶

Overall, the mathematical and phantom studies concluded that online, attenuation-based, tube current control systems showed a significant potential for clinical dose reduction without compromising image quality. Furthermore, the reduction in tube current would reduce x-ray tube load and thus result in lower operational costs of CT scanners.⁶

Clinical Studies in Tube Current Modulation

Multiple clinical studies have been published using Z-axis tube current modulation (AutomA on GE scanners). The majority of these studies come from the Radiology Department at Massachusetts General Hospital.⁷⁻⁹ As previously mentioned, the GE AutomA system requires an input of the noise index, as well as maximum and minimum tube current thresholds. These thresholds make sure that tube current remains in a usable range during the entirety of the scan without unexpectedly high outputs through regions in order to maintain the constant noise index.⁷

One such clinical study involved utilizing tube current modulation in abdominal and pelvic CT exams with a sixteen slice scanner.⁷ Sixty-two patients underwent follow-up

abdominal CT scans using Z-axis modulation. These images were then compared with previous images obtained using fixed tube current techniques from the same patients, but otherwise using identical imaging parameters. The mean interval between the scans was 5 months (range 2-8 months). The two sets of images were graded by subspecialty radiologists on the basis of diagnostic acceptability and image noise. Images were graded on a five point scale with 1 being unacceptable, 3 being acceptable and 5 being excellent. Images at five anatomic levels in the abdomen and pelvis were used, including the upper liver at the level of the diaphragm, the porta hepatic, right kidney hilum, iliac crest, and upper margin of acetabulum. The total mAs for each exam was also recorded for comparison.⁷

The results of the abdominal-pelvic study ([Table 1-2](#)) showed that scores for image noise and diagnostic acceptability of images at the levels of the upper liver and the acetabulum were slightly lower with Z-axis modulation then compared to fixed tube current scans, although the results were not statistically significant ($p = 0.34$). At all other levels there were no significant differences in the scores for image noise and diagnostic acceptability between the two techniques. Any lesions detectable on the manual tube current scans were also detectable on the Z-axis modulation scans. An average overall mAs reduction of 31.9% (range 18.8% to 87.5%) was found for Z-axis modulated scans compared to fixed tube current techniques ([Table 1-3](#)). The use of Z-axis modulation resulted in an mAs reduction in 87% of all exams. An increase in mAs was found in 13% of exams using Z-axis modulation and is attributable to the larger mean weight of patients in this category as compared to those patients that had reduced mAs. Although mAs increased in these exams, a significant ($p = 0.1$) improvement in image noise and diagnostic acceptability was noted for all cases. This fact shows that previous scans with overweight patients possibly utilized inappropriately low tube currents resulting in below

average image quality. Overall, the study showed that significant dose reduction is possible with Z-axis modulation and highlighted the need for proper technique settings of both the minimum and maximum current limits in order to ensure appropriate noise levels in images.⁷

Another clinical test performed by the same group evaluated dose reduction and scanner performance in the detection of urinary tract stones using Z-axis modulation.⁸ This study used both phantom and patient studies. In the phantom study, sixteen calcium oxalate or calcium phosphate kidney stones were embedded in the collecting systems of two freshly harvested bovine kidneys. The size of the stones ranged from 2.5 to 19.2mm. The kidneys were placed in an elliptical Plexiglas container that was then filled with a physiologic saline solution. The phantom was scanned on a Siemens 16 slice CT scanner six times. The phantom was scanned once with a fixed tube current technique, and then once with Z-axis tube current modulation at 5 different noise index settings; 14, 20, 25, 35, and 50. The remaining scanning and reconstruction parameters were kept the same for all scans. The phantom images were then viewed by two separate radiologists who were blinded to the scanning techniques and graded using the same 5 point scale described above to describe the detectability of the stones in the images.

In addition to the phantom study, patient studies were conducted in 22 patients using Z-axis modulation. As in the previously described study, all patients had been previously scanned using standard fixed current techniques with all other scanning parameters kept the same. The same two radiologists evaluated both sets of images using the same five point scale for conspicuity and margins around the stones.

In the phantom study, both radiologists identified all 16 stones in the fixed tube current technique images, as well as in the Z-axis modulated images at noise indexes of 14, 20, and 25. Three stones smaller than 5 mm were not identified by either radiologist in images from Z-axis

modulation with a noise index of 35 and 50. There was no significant difference ($p > 0.5$) in stone conspicuity, image noise, or diagnostic acceptance between fixed current and Z-axis modulated images at a noise index of 14, 20 or 25.⁸ Dose reduction, by means of reduced mAs, was found in all Z-axis modulated scans ranging from 51% in the noise index 14 case, to 92% in the noise index 50 case, although as previously mentioned, not all stones were localized with this technique. An mAs reduction of 76% was found in the noise index 25 case, the highest noise index where all stones were detected.⁸ Kidney phantom images at each noise level are shown in [Figure 1-7](#).

Similar dose reductions were found in the patient studies, although only noise indexes of 14 and 20 were used. All stones located with the fixed tube current scans were also located with Z-axis modulation, and no statistically significant difference ($p > 0.7$) was found in the radiologists ratings for conspicuity, image noise, or diagnostic acceptability.⁸ An overall reduction in mAs of 43% was found with a noise index of 14, and a 66% reduction was found at a noise index of 20.

Overall the study demonstrated that doses in urinary tract stone detection exams can be greatly reduced by utilizing Z-axis modulation techniques. These reductions can be higher than in the cases of chest or abdominal imaging due to the high contrast nature of urinary tract stones in soft tissue, allowing for slightly noisier images than required for low contrast detection cases.⁸ It was also found that for these exams, a 5% reduction in the noise index correlates to a dose (mAs) increase of approximately 10%.

The same research group conducted a similar study of chest CT studies comparing fixed tube current methods to Z-axis modulation.⁹ Very similar methodologies were used as in both the previous studies. The study used 53 patients, with two radiologists reading the results of CT

exams and rating them based on image noise, diagnostic acceptability and streak artifacts. Again the study found that Z-axis modulation provided acceptable imaging of the chest, including lung parenchyma and mediastinal structures, with no significant differences in image noise, diagnostic acceptability, or streak artifacts, as compared to fixed tube current techniques.⁸ The use of Z-axis modulation showed average mAs reductions of 18%, 26%, and 38%, with a noise index setting of 12, 12.5, and 15 respectively, when compared to fixed tube current protocols. Again tube current was found to increase slightly in heavier patients, which is a result of the system attempting to keep image noise constant throughout the thicker area of the scan. It was noted that care should be taken by physicians to pay special attention to noise requirements from larger patients to avoid unnecessary increases in dose.⁸

Current State of the Art

While all previous mentions of tube current modulation have been with respect to either angular or Z-axis techniques, there are CT scanners currently available that make use of both systems simultaneously. This technology is currently only available from high-end, top of the line scanners, but is expected to trickle down and become more prevalent in the industry as time progresses. A study has been published¹⁰ in which a Siemens Somatom Sensation 16 scanner was used to compare the combined modulation technique with angular modulation and fixed tube current modes of operation (CARE Dose 4D). In this scanner, a scout image performs the normal task of assigning tube currents for each slice along the Z-axis in order to maintain constant image noise. While the scan is in progress, the tube current is modulated as the tube rotates around the patient in order to adjust photon flux to match patient specific attenuation for each projection angle. This combined modulation is referred to as xyz modulation. In this particular study 152 patients were used who underwent contrast enhanced CT examinations of the abdomen and pelvis. Seventy-nine patients were scanned using xyz-axes modulation with

forty-two using the weak decrease-strong increase operation mode, and thirty-seven using the average decrease-average increase operation mode (explained below). Forty-two patients were then scanned using only the angular modulation technique, and thirty-one patients were scanned using a fixed tube current technique.

As with the GE system, a user input of an acceptable noise level is required, along with a Siemens specific modulation characteristic for slim or obese patients. This modulation setting differs based on patient size, and decreases tube current for slim patients and increases current for obese patients. The extent to which the tube current is increased or decreased can be controlled via the setting of modulation strength, classified as either strong, average, or weak. A strong setting for obese patients results in a larger increase in dose corresponding to lower image noise, while a weak setting for an obese patient spares patient dose at the expense of increased image noise. For slim patients, a strong modulation setting results in more image noise and lower patient dose, while a weak modulation setting results in higher dose and less noise.¹⁰ It is this author's opinion that the method for noise level selection employed by Siemens is infinitely more complex than that set by GE for Z-axis modulation, and could result in improper technique settings by technologists.

As in the previous clinical studies, images from each set of patients were graded by two radiologists on the basis of image noise, diagnostic acceptability, streak artifacts, and visibility of small structures. A quantitative measure of image noise was also recorded for each exam in the liver parenchyma at the level of the porta hepatis.

The study found no significant statistical difference in the weights ($p = 0.3$) or ages ($p = 0.5$) of patients in each of the scanning technique groups.¹⁰ In evaluating values of image quality parameters (radiologist measured), there was no significant difference found for examinations

performed with fixed tube current, angular modulation, and weak decrease-strong increase method combined modulation . The scores from the average increase -average decrease method of combined modulation were found to be significantly lower than other techniques however ($p = 0.0001$). Of these examinations, several were labeled as below diagnostic quality with more than acceptable image noise. In comparing objective image noise, again there was no significant difference in values for exams performed with fixed tube current, angular modulation, and weak decrease-strong increase combined modulation. Again, the noise values for average increase-average decrease mode of combined modulation were significantly higher than any other technique ($p > 0.1$).

In comparing doses measured for each technique, a significant reduction ($p < 0.0001$) was found in the angular and combined methods of tube current modulation. Compared to fixed current techniques, there was an average dose reduction of 19% for angular modulation technique exams, and 42% for weak decrease-strong increase combined modulation exams. The average decrease-average increase method of combined modulation resulted in 44% average dose reduction, although at the expense of image quality as previously mentioned. It should be noted that dose changes in this study were reported as changes in $CTDI_{vol}$ and not in mAs as reported in previous studies, making a direct comparison between studies impossible.

The combined modulation technique study showed the increased dose savings of combining angular and Z-axis tube current modulation, but also highlighted the importance of proper technique settings correlating to patient size.

Conclusions

As has been discussed, tube current modulation techniques represent technological advances in CT scanners that allow for a reduction of patient dose while maintaining image quality. Three methods have been described for tube current modulation; angular modulation,

which modulates tube current in the x-y plane as the tube rotates around the patient, Z-axis modulation in which tube current remains constant for a give rotation, but changes as the patient advances though the scanner, and xyz modulation, which combines the two techniques.

Mathematical simulations as well as phantom and patient studies have shown the dose reduction benefits of current modulation, and dose reductions for both angular and Z-axis modulation have been shown to be comparable for similar examinations. Combined tube current modulation makes use of the advantages of each method to further reduce patient doses, but at the present time is only available on high end scanners.

While tube current modulation can provide numerous benefits to clinical CT examinations, it is not without its drawbacks. While the basic principles in use by different manufacturers remains similar, the method of implementation can vary greatly between scanners, which can make clinical use in a clinic with multiple manufacturers difficult. The lack of uniformity between vendors, as evident with the noise index value of GE compared to the decrease-increase method of Siemens, makes technologist training and understanding of the technology paramount to proper diagnostic use of the equipment, as any dose savings in a single scan are nullified if scans must be repeated due to improper techniques.

Purpose of Study

The benefits and limitations of tube current modulation systems in CT scanners have been discussed, but as of now there is no simple method for medical physicists to ensure proper functionality of such systems from a quality assurance standpoint. An improperly functioning tube current modulation system would obviously pose numerous problems to a radiology department, including the possibility of unacceptable image quality as well as unknowingly higher patient doses. The purpose of this body of work was to develop a simple, effective method to test the functionality of in-plane tube current modulation systems in order to ensure proper

clinical operation. Variations in performance of the system could be tracked on a monthly basis, and proper maintenance or repairs could be requested if system parameters vary to an unacceptable level.

Overview

A preliminary idea to test the functionality of an in-plane tube current modulation system was to create a series of elliptical tissue equivalent phantoms of the same minor axes, but with varying major axes. The overall concept was that such phantoms could all be scanned using the same image quality setting of the tube current modulation system, and the respective image noises from each phantom scan should be similar, regardless of major axis length. Similar image noise values for varying sized phantoms would show that the in-plane tube current modulation was indeed varying tube current based on attenuation values in order to maintain a constant image noise. If image noise values were found to vary greatly for different sized phantoms, one could assume something was wrong with the modulation system. Such a test would be easy to perform, take little time, and the results could be recorded for long term tracking of scanner performance.

Approach

We decided to use existing CT image quality and dose measurement phantoms for the study, and to develop tissue equivalent elliptical attachments. This was chosen in the interest of using less material and for the flexibility in allowing for dose, as well as image quality measurements to be taken without having to manufacture two sets of phantoms.

In order to fabricate such elliptical phantoms, a tissue equivalent material was developed. This material was to have a density similar to that of soft tissue (1.04 g/cm^3), as well as similar x-ray attenuation properties in the diagnostic energy range (80-120 kVp) used in CT imaging. The developed material was also desired to be flexible and compressible in order to maintain

close contact with the existing CatPhan (The Phantom Laboratory, Salem NY) and standard CTDI head phantom, as well as for applications in other phantom development projects dealing with mammography and anatomic tomographic phantoms.

Once such a tissue equivalent material was developed, a series of five elliptical phantoms was created. All phantoms had a minor axis of 16cm, corresponding to the diameter of commercially available CTDI and CatPhan phantoms. The major axes of the created phantoms ranged from 26 to 37.5 cm.

The created phantoms were then used with a Siemens Somaton Sensation 16 slice scanner equipped with CareDose4D[®] tube current modulation system. This system uses angular as well as Z-axis modulation to adjust tube output on the fly within a single tube rotation as well as along the length of the scan based on a pre-examination topogram. Both of these systems work together to ensure uniform image noise throughout a CT scan, while reducing patient doses as compared to fixed tube output protocols. The user input for image noise has changed slightly from that mentioned in the studies above. The user input for the CareDose4D[®] software is now a single reference mAs value and the strong, normal, and weak modifications are no longer used. The reference mAs value corresponds to the mean effective mAs value that the system will use for a “reference patient” with the same protocol. The reference patient is described by Siemens as a typical adult weighing 155-180 pounds for adult protocols, and a typical child weighing 45 pounds for children’s protocols. Based on the reference mAs value, the system adapts the tube current to the individual patient size. A higher reference mAs setting indicates a higher tube current used in order to produce less image noise in the reconstructed image. A lower reference mAs setting can be used for lower patient dose in scans where image noise is not of crucial importance.

Each of the created phantoms was imaged with the Siemens CT system at six different reference mAs values. These reference values were taken for a standard adult abdominal routine at values above and below the default setting. The pixel uniformity values for each phantom at each setting were then plotted in order to determine proper functionality of the angular component of the CareDose 4D tube current modulation system, as well as general trends in dose and image quality.

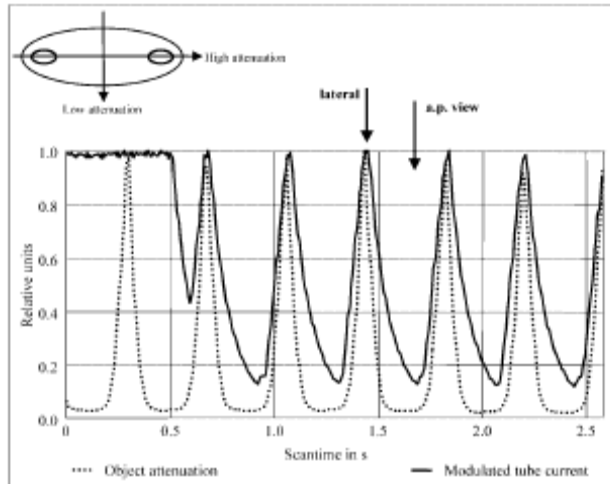


Figure 1-1: Phantom demonstration of angular tube current modulation. Tube current remains constant for the first 180 degrees rotation about the shoulder phantom before being modulated to match attenuation.

Reprinted with permission from
 C. Suess, and X. Chen, "Dose Optimization in Pediatric CT: current technology and future innovations," *Pediatr. Radiol* **32**, 729-734 (2002).

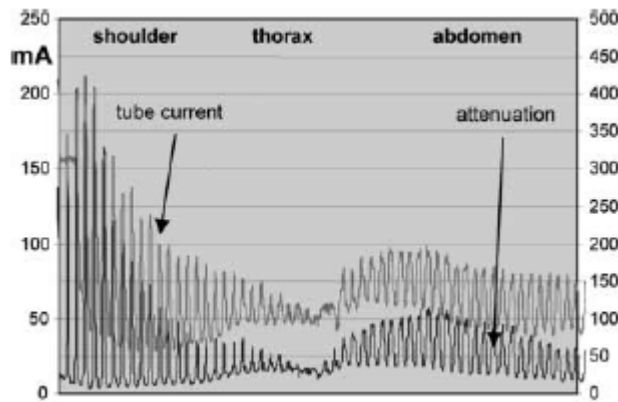


Figure 1-2: Real-time tube current modulation. Tube current is adjusted in real time to match patient attenuation. Larger currents are needed through the shoulder region with less required through the thorax due to lower attenuation.

Reprinted with permission from
 C. Suess, and X. Chen, "Dose Optimization in Pediatric CT: current technology and future innovations," *Pediatr. Radiol* **32**, 729-734 (2002).

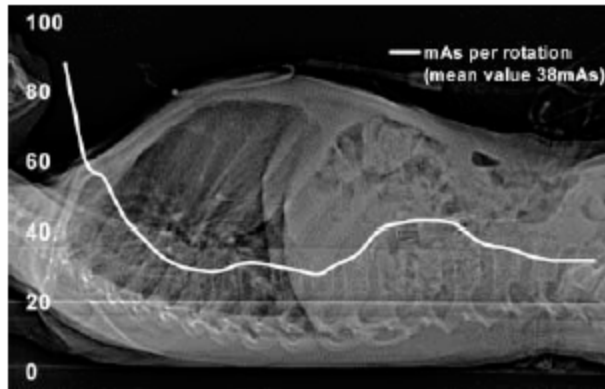


Figure 1-3: Z-axis modulation. A scout radiographic image is used to determine the appropriate mAs per rotation based on patient attenuation characteristics.

Reprinted with permission from
C. Suess, and X. Chen, "Dose Optimization in Pediatric CT: current technology and future innovations," *Pediatr. Radiol* **32**, 729-734 (2002).

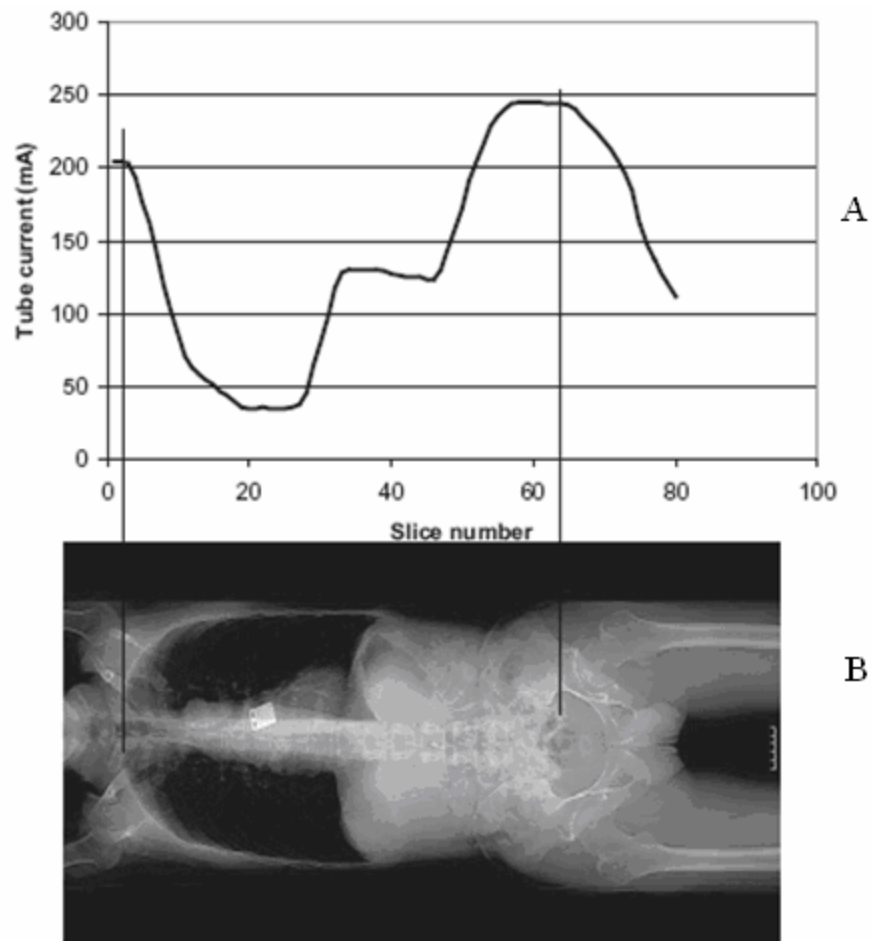


Figure 1-4: Z-axis modulation. Tube current (A) varies per slice as determined by a scout radiograph (B).

Reprinted with permission from

J. Althen, "Automatic Tube current Modulation in CT- A Comparison between Different Solutions," *Radiation Protection Dosimetry* **114**, 308-312 (2005).

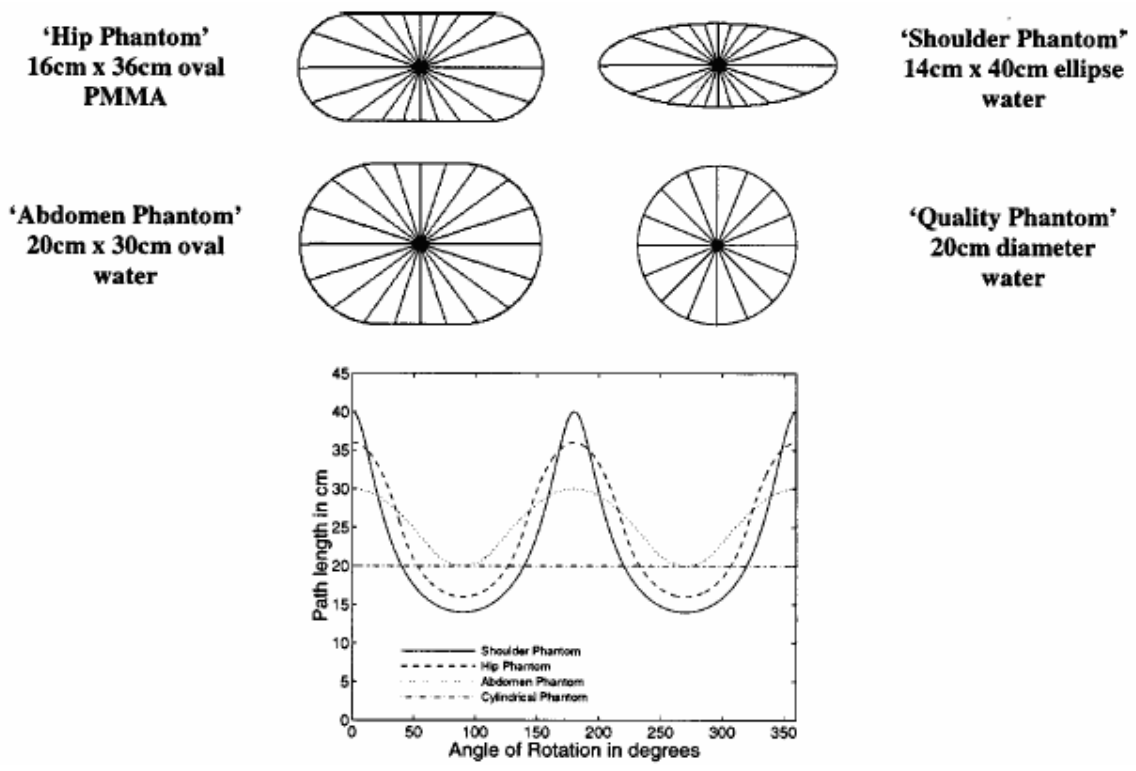


Figure 1-5: Summary of phantoms and associated path-lengths. A) Phantom shapes used in simulation studies B) path-length as a function of angle of rotation for each phantom, demonstrating attenuation differences for noncircular shapes.

Reprinted with permission from

M. Geis, W. Kalender, H. Wolf, and C. Suess, "Dose Reduction in CT by Anatomically Adapted Tube current Modulation I Simulation Studies," *Med. Phys* **26**, 2235-2247 (1999).

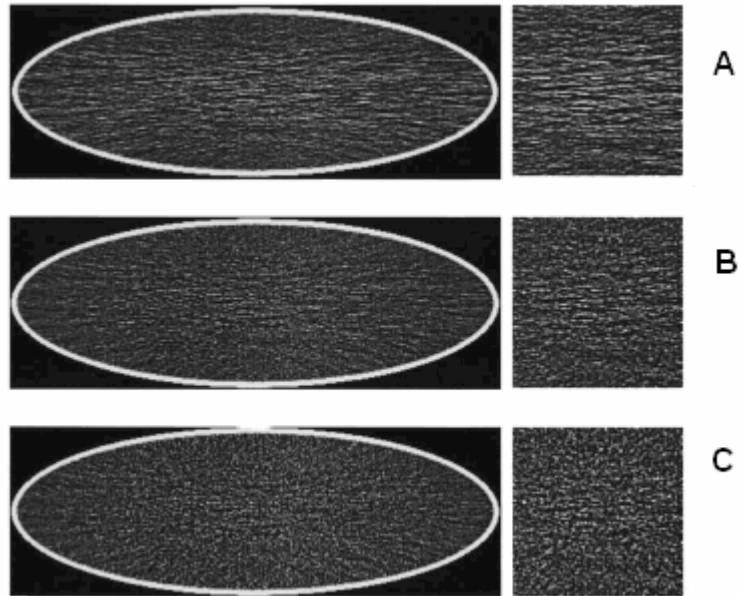


Figure 1-6: Image noise as a function of modulation parameter. A) With no modulation anisotropic noise is visible in the direction of highest attenuation. B) Modulation according to the square root of attenuation: minimizes noise but anisotropic effects are still visible. C) Modulation according to attenuation, slightly higher noise than b, but isotropic.

Reprinted with permission from
M. Geis, W. Kalender, H. Wolf, and C. Suess, "Dose Reduction in CT by Anatomically Adapted Tube Current Modulation I Simulation Studies," *Med. Phys* **26**, 2235-2247 (1999).

Table 1-1: Results of phantom dose reduction studies

TABLE I. (a) Comparison of dose reduction using a cylindrical, oval and elliptical water phantom, and two modulation types. (Scan parameters: 120 kV, 5 mm, 1 s, 70% modulation amplitude.) (b) Dose reduction values for the shoulder phantom obtained by simulations (Ref. 1). (Scan parameters: 120 kV, 5 mm, 1 s, 70% modulation amplitude.)

Phantom	Modulation type	Sigma in HU	Measured mAs	Normalized mAs	Dose reduction in %
(a)					
Cylindrical water phantom 20 cm diam	None (const. mA)	2.9	494	494	0.0%
	Sinusoidal	2.9	491	491	0.6%
	Attenuation-based	2.9	487	487	1.4%
Oval water phantom 20 cm×30 cm	None (const. mA)	5.7	493	493	0.0%
	Sinusoidal	6.1	393	450	9.7%
	Attenuation-based	6.1	367	420	11.8%
Shoulder phantom without inserts 14 cm×40 cm	None (const. mA)	19.0	213	213	0.0%
	[Fig. 4(a)]				
	Sinusoidal	14.6	213	126	34.1%
	[Fig. 4(b)]				
	Attenuation-based	13.2	220	103	44.6%
	[Fig. 4(c)]				
(b)					
Oval water phantom 20 cm×30 cm	None (const. mA)				0.0
	Sinusoidal				9.4
	Attenuation-based				9.5
Shoulder phantom without inserts 14 cm×40 cm	None (const. mA)				0.0%
	Sinusoidal				29.7%
	Attenuation-based				39.3%

Reprinted with permission from
W. Kalender, H. Wolf, and C. Suess, “Dose Reduction in CT by Anatomically Adapted
Tube Current Modulation II Phantom Measurements,” *Med. Phys* **26**, 2248-2253 (1999).

Table 1-2: Comparison of image noise and diagnostic acceptability

Anatomic Level	Z-Axis Modulation		Fixed Tube current	
	Image Noise	Diagnostic Acceptability	Image Noise	Diagnostic Acceptability
Upper Liver	2.8 +/- 0.7	3.0 +/- 0.6	2.9 +/- 0.7	3.1 +/- 0.8
Porta hepatis	2.9 +/- 0.6	3.2 +/- 0.6	2.8 +/- 0.7	3.2 +/- 0.7
Renal hilum	2.8 +/- 0.7	3.2 +/- 0.7	2.7 +/- 0.7	3.2 +/- 0.7
Iliac crest	3.0 +/- 0.8	3.3 +/- 0.6	2.9 +/- 0.7	3.4 +/- 0.7
Acetabulum	2.9 +/- 0.7	3.3 +/- 0.6	3.0 +/- 0.7	3.4 +/- 0.5

Note- Data are means and standard deviations. No statistically significant differences were found between CT images acquired with Z-axis automatic modulation and those acquired with fixed tube current (P = .34-.84)

Reprinted with permission from

W. Kalender, H. Wolf, and C. Suess, "Dose Reduction in CT by Anatomically Adapted Tube Current Modulation II Phantom Measurements," Med. Phys **26**, 2248-2253 (1999).

Table 1-3: Reductions in tube current time product with Z-axis modulation

Anatomic Level	Tube Current-Time Product	Tube Current-Time Product	Tube Current-Time Product
	with Z-Axis Modulation	with Fixed Tube Current	Reduction with Z-Axis Modulation*
Upper Liver	103.6 +/- 50.3	187.9 +/- 21.4	84.3 +/- 45.7 (44.9)
Porta hepatis	121.0 +/- 51.6	187.9 +/- 21.4	66.9 +/- 47.7 (35.6)
Renal hilum	119.9 +/- 54.2	187.9 +/- 21.4	68.0 +/- 49.4 (36.2)
Iliac crest	115.4 +/- 56.4	187.9 +/- 21.4	72.5 +/- 51.7 (38.6)
Acetabulum	123.8 +/- 50.0	187.9 +/- 21.4	64.1 +/- 47.1 (34.1)

Note- Data are mean milliampere-seconds +/- standard deviations

* Data in parentheses indicate percent change. For examinations in which mean tube current time product decreased with Z-axis modulation compared with fixed tube current, the difference was statistically significant (P<0.001)

Reprinted with permission from

W. Kalender, H. Wolf, and C. Suess, "Dose Reduction in CT by Anatomically Adapted Tube Current Modulation II Phantom Measurements," Med. Phys **26**, 2248-2253 (1999).

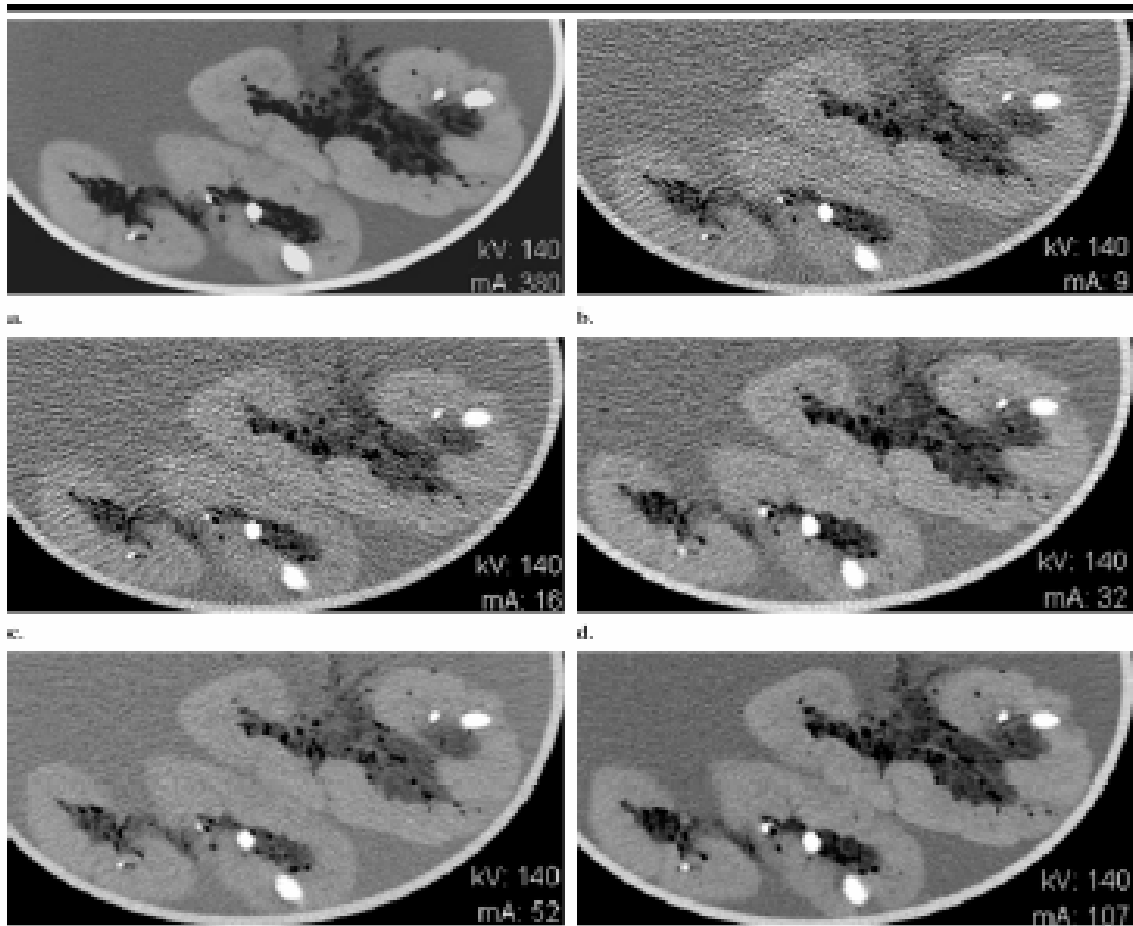


Figure 1-7: Kidney phantom. Kidney stones visualized in bovine kidneys scanned with a) fixed tube current technique, b) Z-axis modulation noise index =50, c) noise index=35, d) noise index=25, e) noise index=20, f) noise index=14. Scans at higher noise indexes show a substantial increase in image noise and lowered diagnostic acceptability.

Reprinted with permission from
 M. Kalra, M. Maher, R. D'Souza, S. Rizzo, E. Halpern, M. Blake, and S. Saini, "Detection of Urinary Tract Stones at Low-Radiation-Dose CT with Z-Axis Automatic Tube Current Modulation: Phantom and Clinical Studies," *Radiology* **235**, 523-529 (2005).

CHAPTER 2 TISSUE EQUIVALENT MATERIAL DEVELOPEMT

The first portion of this work centered on the development of a flexible, compressible, tissue-equivalent material for use in radiological phantom construction. The material was to be equivalent to human soft tissue in density and x-ray attenuation properties in the diagnostic energy range (80-120 kV). Phantoms previously created by the lab have been epoxy based, giving them a solid consistency similar to acrylic. While the epoxy based material was tissue equivalent, it was difficult to work with and limited in its scope of use. It was also hoped that the new compressible material could be used for applications in more realistic mammography phantoms to better model breast tissue properties under clinical conditions.

Acrylic was used as a benchmark for comparison of the attenuation properties of the created material. Acrylic has previously been used for commercially available phantoms due to its similar x-ray attenuation properties in the diagnostic energy range. The density of acrylic is 1.17 g/cm^3 though, and as such the density of acrylic was not used as a benchmark for the phantom material development. A target density of 1.04 g/cm^3 , the density of human soft tissue, was used as a target density value.

Silicone-Based Rubber Material Testing

EcoflexTM, a silicone-based rubber compound produced by Smooth-On Inc. (Easton PA), was first tested for its utility in creating a compressible tissue equivalent phantom material. EcoflexTM consists of two parts, A and B, which are mixed in a 1:1 ratio by weight and allowed to cure for 12 hours to produce a stretchy, compressible material that returns to its original form after deformation. Preliminary tests showed the compressibility of EcoflexTM was as desired and it had a published density (1.07 g/cm^3) close to that of soft tissue (1.04 g/cm^3). Based on these preliminary tests, molds were produced in order to better quantify the properties of the material.

Sample Preparation

Epoxy molds were constructed in order to make slabs of Ecoflex™ of a reproducible thickness. Solid pieces of epoxy were poured and allowed to harden overnight. Cutouts were then machined into the epoxy slabs with a Vision Pro Engraver (Dade City, FL) to create four 10x10 cm square molds with a depth of approx 1 cm. Using these molds, slabs of Ecoflex™ were poured with various additives in order to test their radiographic attenuation and density properties. Pictures of the epoxy molds and the Ecoflex™ slabs are shown in [Figure 2-1](#).

Additives used included phenolic microspheres (System Three, Auburn WA), powdered calcium carbonate, and powdered polyethylene (Fisher, Fairlawn NJ). The by-weight percentages of additives used in the samples are given in [Table 2-1](#). The Ecoflex™ material easily peeled out of the molds and did not require the mold release previously needed with epoxy based tissue equivalent materials, making sample preparation clean and simple as compared to epoxy based materials.

Sample Testing

After the previously mentioned samples were mixed, poured, and cured, they were tested for density and radiographic attenuation properties. As mentioned, a density of 1.04 g/cm^3 , the density of soft tissue, was used for a target density. A 1.25 cm thick Acrylic slab was used as a benchmark for attenuation properties as acrylic is commonly used in commercial phantom production. A portable x-ray generator (Source-Ray Inc. model SR-115, Boheimia NY) and CCD detector were utilized for testing the attenuation properties of the samples. The samples were placed directly on the CCD detector, and two slabs of Ecoflex™ based material, the acrylic slab, and a piece of BR-12 breast tissue equivalent tissue were imaged at a time. The average pixel values from a 156x156 pixel square in the center of each sample for each of three images was taken and then averaged in order to provide a relative comparison of the attenuation

properties of each material. If an Ecoflex™ based slab had an average pixel value similar to that of acrylic, its radiological attenuation properties were in the range required. All images were acquired with an SID of 43 cm, and at 80kVp and 4mA. A sample of the collected x-ray images is shown in [Figure 2-2](#).

Upon inspection, it was found that all prepared Ecoflex™ samples had a much lower average pixel value than acrylic, indicating a higher attenuation of the incoming x-ray beam (it should be noted that the CCD detector utilized assigns pixel values oppositely to that of a conventional digital radiographic unit, in that darker areas represent areas of higher attenuation and lighter areas indicate regions of lower attenuation). The results of the attenuation testing can be found in [Figure 2-3](#). Even the Ecoflex™ samples with up to 10% by weight phenolic microspheres, a low atomic number material added to reduce the density and attenuation of the sample, had substantially higher attenuation values. Density tests were not performed on the Ecoflex™ samples since it was apparent that the material could not successfully be used as a base in tissue equivalent materials due to the high attenuation attributed to its silicone base.

Urethane-Based Rubber Material Testing

After it was realized that Ecoflex™ was unsuitable for use as a base in tissue equivalent materials, other solutions were explored. A range of urethane based compounds with varying material properties were ordered from Smooth-On for further testing. The product numbers and properties of the tested materials can be found in [Table 2-2](#).

These materials were selected from multiple other products based on the listed properties. A larger value for elongation at break, as well as a lower hardness value indicates a more compressible material. All rubbers come in two parts which must be mixed in proportion. A mix ratio of 1:1 by weight was desired for precision and ease of use in preparing samples, but other

options were tested in case their other properties ended up justifying a slightly more complex mixing process. Some materials were offered in both a “wet” and “dry” option, with the “wet” having a built in release agent to aid in the de-molding of plasters or concrete, the intended use of the products. When available, the dry option was chosen but the PMC 121/50 material was available in only a wet option. All materials had a similar de-mold time, which required overnight curing before samples could be removed from their molds.

The same epoxy molds used for making Ecoflex™ slabs of similar thicknesses were utilized to produce slabs of the urethane based materials. Each material was mixed as per its instructions and with no additives in order to compare their base x-ray attenuation values to that of acrylic. Based on these tests, the best material were selected and further tested with various additives in order to reach the desired tissue equivalent properties. Slabs of each of the urethane based materials are shown in [Figure 2-4](#).

Material Testing

Unlike the previously described Ecoflex™ sample testing, where CCD images were taken and pixel values compared, a new approach was taken for ease of calculations and comparison in testing the urethane based materials. A Keithley 35050A ion chamber (Cleveland, Ohio) was used with a portable x-ray unit (Source-Ray Inc. model SR-115) to measure attenuation through each sample. The ion chamber was suspended on a stand to prevent backscatter effects from altering data, and the slabs of material were placed approximately 18 inches above the chamber on the stand. The beam was collimated so as to not interact with the metal arms of the stand holding the samples, and to fall across the active region of the detector. A tube current of 80 kVp was used with 400 mAs and an SID of 38” for all measurements. The experimental setup can be seen in [Figures 2-5](#) and [2-6](#).

For testing, an initial exposure measurement was taken of open air with no slab in place. Three exposure measurements were then taken each with an acrylic slab, a BR-12 breast tissue equivalent material, and each of the Smooth-On urethane compounds in place above the ion chamber. Based on the measured exposures and slab thicknesses for each material, a relative attenuation coefficient was calculated using Equation 2-1.

$$R=R_0*e^{-u*t} \quad (\text{Eq. 2-1})$$

With:

R = the average measured exposure (R)

R₀ = the initial exposure with no slab in place (R)

u = relative attenuation coefficient (cm⁻¹)

t = the slab thickness (cm)

These relative attenuation coefficient values allow for easy comparison of x-ray attenuation properties between materials and allow slabs of slightly differing thicknesses to be quantitatively compared.

Density measurements of each sample were then taken utilizing Archimedes's principle. A dry sample of each material was weighed on a scale with 0.001 gram precision. The samples were then weighed submerged in a beaker of de-ionized water. Using both these measurements, as well as the known density of the de-ionized water, the density of each sample was calculated using Equation 2-2.

$$\text{Dry weight} / [(\text{dry weight-wet weight})/\text{density of H}_2\text{O}] \quad (\text{Eq.2-2})$$

Results of Attenuation and Density Testing

The results of the initial round of material testing are shown in [Figure 2-7](#) and [2-8](#). Based on these tests, the 121/30 material was selected for use as a base in the tissue equivalent material. It was chosen based on its density and attenuation values being within a reasonable range of that of the desired values of both acrylic and BR-12, a breast tissue equivalent material. It was hoped

that the 121/30 material could be successfully used to develop both a soft tissue and breast tissue equivalent phantom material. The individual attenuation and density properties can be altered by the addition of additives such as phenolic microspheres, calcium carbonate, and polyvinyl chloride in order to reach the desired target values. The 121/30 material was also chosen because its elasticity and compressibility were qualitatively determined to be the best of the group of materials. Other materials such as PMC 744 were found to be extremely firm and not compressible enough. The PMC 121/50 wet material had an oily residue upon firming which was not suitable for long term phantom use if only because of the messy residue it left on anything it came into contact with.

Materials Testing with PMC 121/30

Once the 121/30 material had been selected, further testing was done utilizing a range of previously described additives in order to get its attenuation and density properties to the desired values. The same procedures for measuring attenuation and density described in the previous section were used for this portion of testing. Multiple slabs of material were poured with varying amounts of microspheres, calcium chloride, and/or polyethylene additives. Once the slabs had cured, their relative x-ray attenuation values were measured using the Keithley ion chamber and the previously described method.

For the first round of testing, the 121/30 material was mixed with 5% by weight each of calcium carbonate, polyethylene, and microspheres to gauge these additives' effects on the properties of the base urethane material. It was decided to try to match attenuation values first, and once that was accomplished to then move to adjust the material's density through further additives.

The results of the first round of testing are shown in [Figures 2-9 and 2-10](#). [Figure 2-9](#) shows that the addition of 5% polyethylene to the 121/30 compound did little to alter the

attenuation, while the addition of 5% phenolic microspheres significantly lowered the attenuation. Both of these materials had a lower attenuation coefficient than that of acrylic. The addition of 5% CaCO₃ increased the attenuation of the 121/30 to a value higher than that of acrylic. This indicated that the addition of a lower by-weight percentage of CaCO₃ would bring the attenuation of the material close to the target value of acrylic.

The measured densities presented in [Figure 2-10](#) show that the addition of CaCO₃ increased the density of PMC 121/30 to the desired value of 1.04 g/cm³. The addition of microspheres and polyethylene lowered the density to less than that of water (~1 g/cm³). The specific densities of these materials were not able to be calculated with the previously described method because, being less dense than water, a wet sample weight could not be calculated since the samples floated. Isopropyl alcohol, which has a density lower than that of water, could have been used to calculate these material's densities, but this was deemed unnecessary since they were below the target value.

Further Testing

Based on the results of the initial 121/30 testing, several new samples were poured with varying amounts of CaCO₃ and microspheres in order to get the material properties closer to tissue equivalent. CaCO₃ was added in order to raise the attenuation coefficient of the material, while microspheres acted to lower both the attenuation and the density. It was hoped that some combination of the two materials would produce a tissue equivalent rubber. A list of the newly created material mixtures is provided in [Table 2-3](#).

The samples were tested for attenuation and density in the same manner as the previous samples. The results of this round of testing are shown in [Figure 2-11](#). The densities of all materials with microspheres added were once again less than 1 g/cm³. The densities of both the 2.5% and 3.2% CaCO₃ samples were 1.03 g/cm³, and the density of the 5% CaCO₃ sample

remained at 1.04 g/cm^3 . These density values indicate that increases on the order of 1% in CaCO_3 to the 121/30 mixture produce relatively small changes in density. Based on these test results, the addition of only CaCO_3 seemed to be the most promising, as these samples had a density and attenuation close to the target values of soft tissue. While samples with added microspheres also had attenuation values both above and below that of acrylic, indicating the ability to zero in on the exact attenuation, their low densities made them unsuitable for a tissue equivalent material.

Given the results of the previous tests, the relative attenuation values of the 2.5% and 3.2% CaCO_3 sample were plotted as a function of their percentage of CaCO_3 , since the samples lay on either side of the target attenuation of acrylic. A linear-fit trend line was then fit to the data points, and used to calculate the percentage of CaCO_3 that would produce the same relative attenuation as acrylic, 0.302 cm^{-1} in this case. This calculation yielded a value of 2.8% CaCO_3 to be added to the PMC 121/30 urethane in order to provide a soft tissue equivalent attenuation coefficient. A sample of 2.8% CaCO_3 was then poured in order to verify this calculation. The attenuation of this 2.8% sample was found to be equal to that of acrylic. Density measurements of the 2.8% CaCO_3 sample showed that it has a density of 1.037 g/cm^3 which is extremely close to the target value for soft tissue and essentially tissue equivalent within bounds of experimental error. It was determined that the combination of x-ray attenuation characteristics and density very close to the ICRP standard for soft tissue was suitable to make the 2.8% by weight CaCO_3 added to PMC 121/30 urethane mixture a suitable tissue equivalent material for phantom construction.

Table 2-1: Ecoflex™ samples prepared with various additives (percentages by weight)

Ecoflex™ - no additives
5% polyethylene
10% polyethylene
15% polyethylene
20% polyethylene
10% CaCO ₃
20% CaCO ₃
5% poly - 5% CaCO ₃
10% poly/10% CaCO ₃
10% microspheres



Figure 2-1: Three tissue equivalent slabs curing in epoxy molds

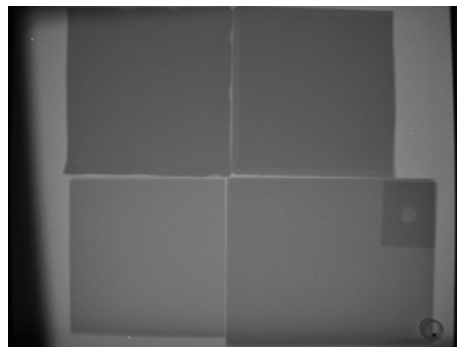


Figure 2-2: Relative attenuation of samples: Two Ecoflex™ based samples on top below a breast equivalent (lower left) and acrylic (lower right) slab.

Attenuation of Ecoflex Based Materials

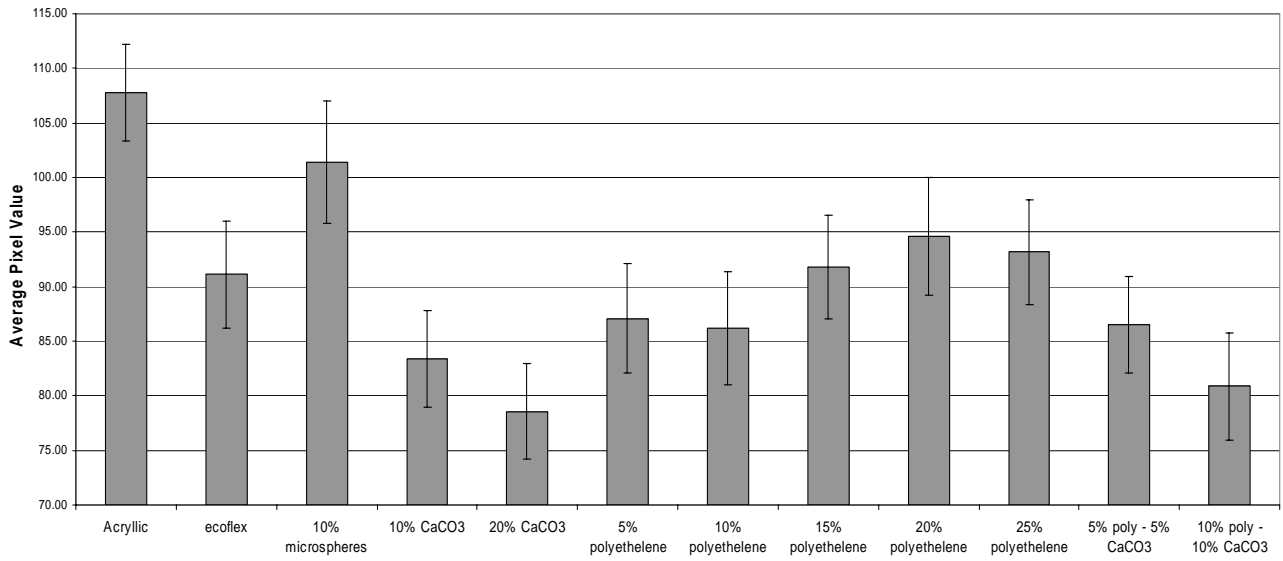


Figure 2-3: Relative attenuation of Ecoflex™ based tissue equivalent materials

Table 2-2: Material properties of various Smooth-On rubbers

Rubber Compound	A:B Mix Ratio	Hardness	Elongation at Break
PMC 780 dry	2:1 by weight	80	700%
PMC 744	2:1 by weight	45	400%
PMC 121/30 dry	1:1 by weight	30	1000%
PMC 121/50 wet	1:1 by volume	50	500%

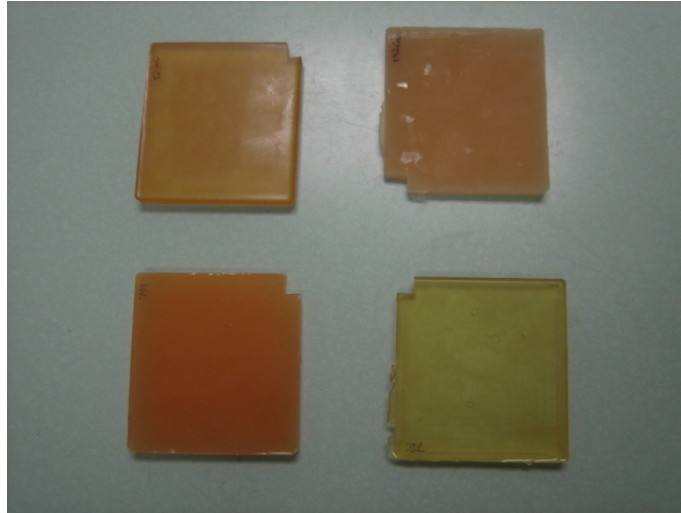


Figure 2-4: Slabs of PMC 780, 744, 121/30 and 121/50 urethane-based rubbers offered by Smooth-On.



Figure 2-5: Experimental setup for attenuation measurement. Slabs of material were placed 18" above an ion chamber.



Figure 2-6: Full experimental setup with portable x-ray generator 38" above the ion chamber.

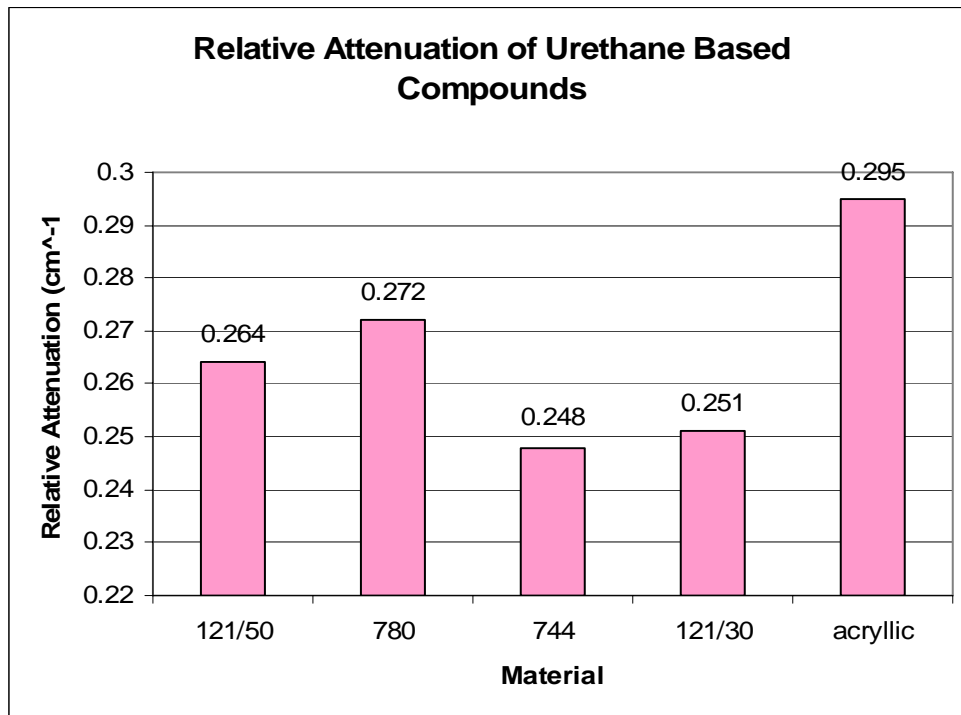


Figure 2-7: Comparison of attenuation coefficients of urethane based rubbers.

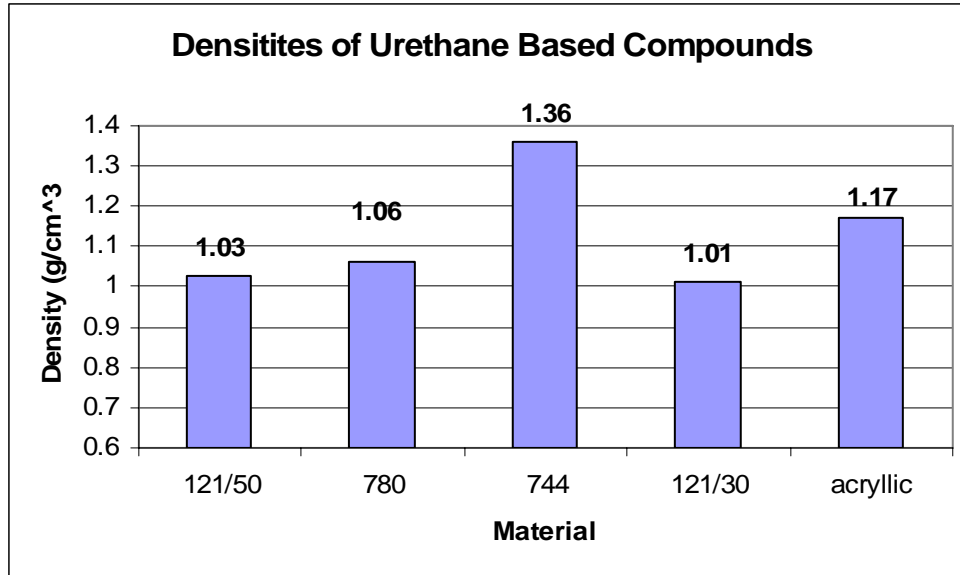


Figure 2-8: Comparison of densities of urethane based rubbers.

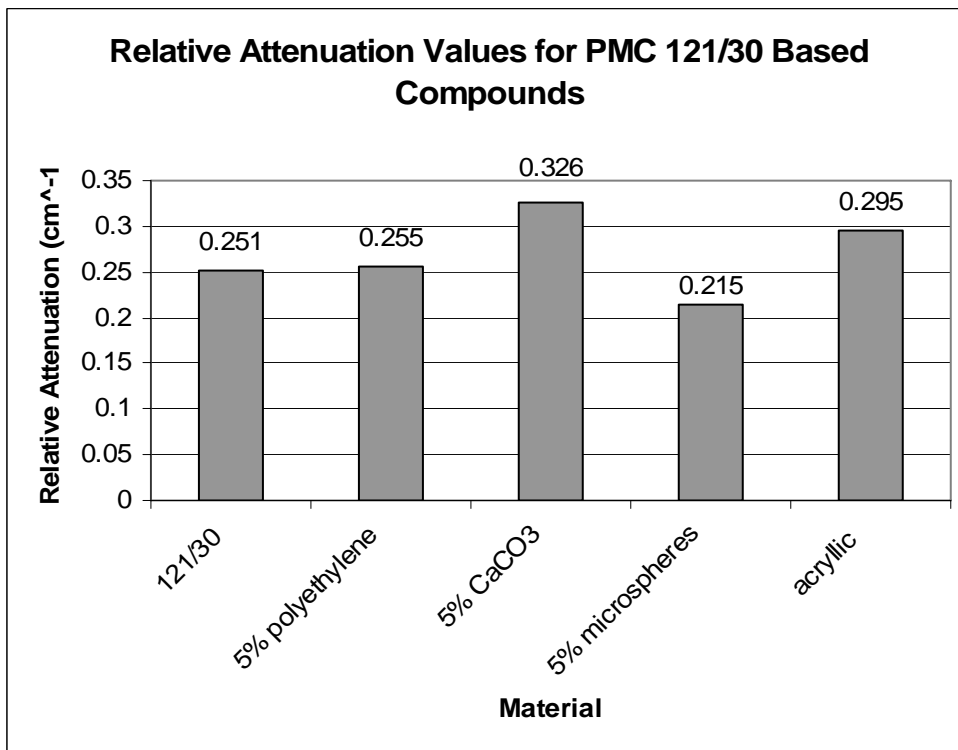


Figure 2-9: Attenuation coefficients of PMC 121/30 based materials.

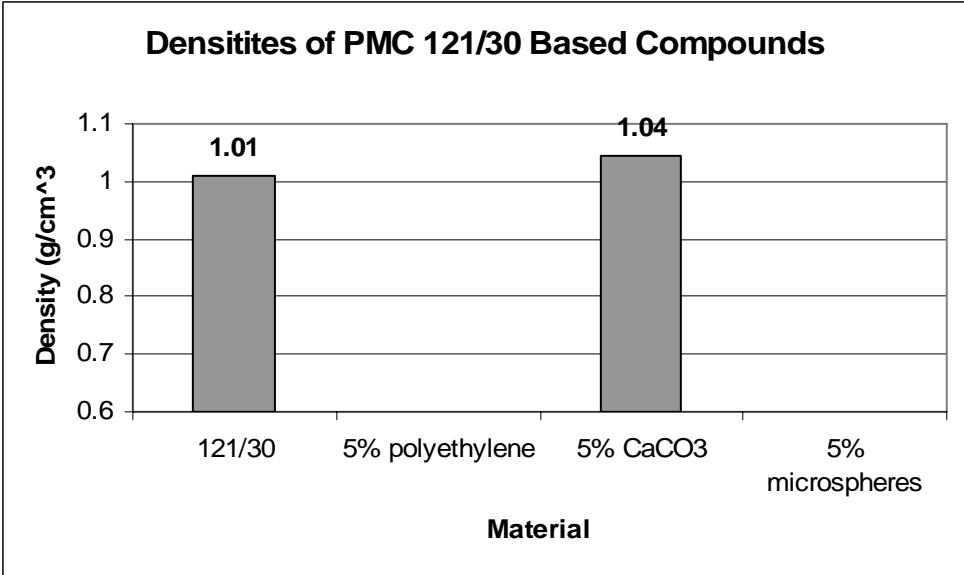


Figure 2-10: Densities of PMC 121/30 based materials

Table 2-3: List of slabs poured with 121/30 as a base (Ca= CaCO₃ & micro =microspheres, percents are by weight)

2.5% CaCO ₃
3.2% CaCO ₃
5% CaCO ₃
2.25% Ca/1% micro
2.25% Ca/2.25% micro
4.5% Ca/ 4.5%micro

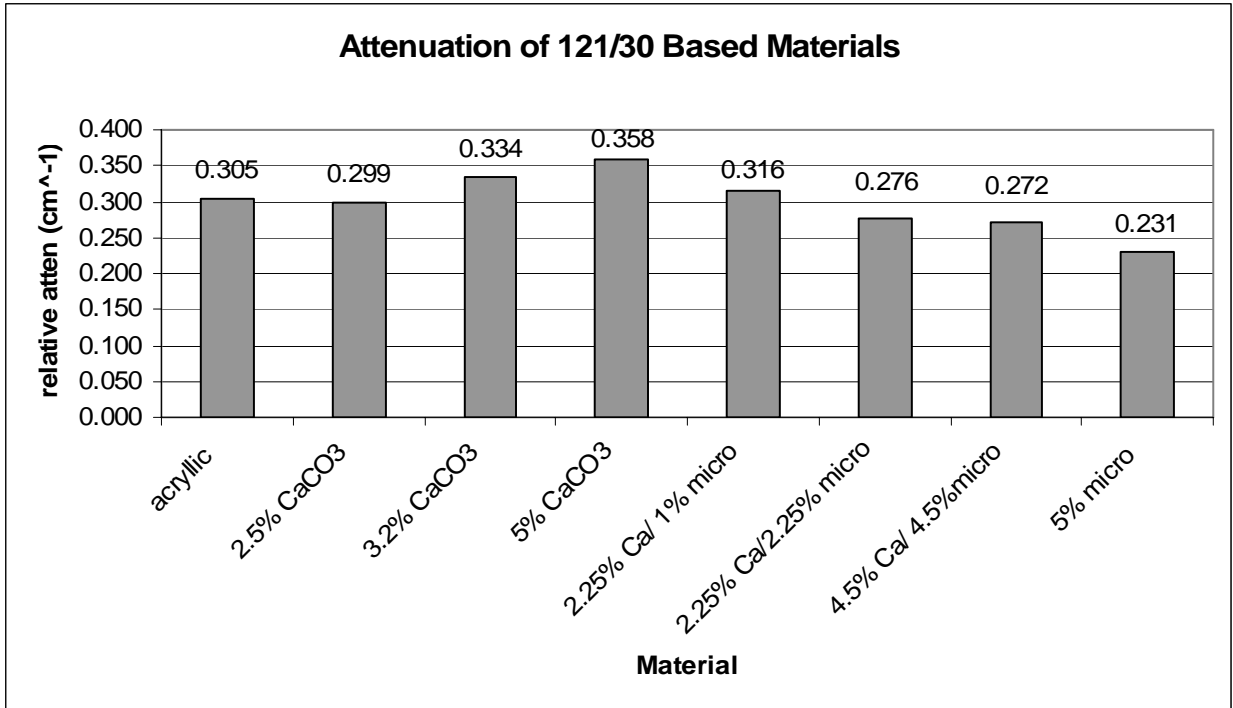


Figure 2-11: Attenuation values of 121/30 with various additives

CHAPTER 3 ELLIPTICAL PHANTOM CONSTRUCTION

Once a tissue equivalent urethane based material was developed, it was used in the construction of several elliptical phantoms. These phantoms were to be used in testing proper functionality of tube current modulation systems in clinical CT scanners. A total of five such phantoms were created, all with a height of 15cm, a minor axis of 16cm, and major axes varying between 26 and 37.25cm. A basic diagram of the proposed phantoms is shown in [Figure 3-1](#). The phantoms were designed to fit an existing CTDI head phantom with a height of 15cm and a diameter of 16cm.

Materials and Methods

The original idea for building the phantoms was to utilize several large pieces of four inch thick packing foam already in the lab as a frame for pouring the phantoms. Elliptical cutouts would be cut into each of three slabs, which would be stacked and then filled with the tissue equivalent rubber. Before constructing the phantoms, small scale testing was done in order to verify the design concept. Two small rectangular cutouts were made in a 4" thick piece of packing foam, and a piece of wax paper was epoxied to the bottom to act as a base. The walls of one cutout were lined with wax paper, while the other was left as bare foam. Both cutouts were filled with the tissue equivalent PMC 121/30 material and left to cure overnight. It was found that the cured rubber easily pulled out of both cutouts. The cutout lined with wax paper produced a sample with cleaner edges, while the sample from the foam cutout was rough and uneven as the liquid rubber material filled in the small voids in the foam.

Based on the small scale test, the first elliptical phantom was constructed. An ellipse with a 26cm major axis and 16cm minor axis was traced onto and cut out of three large slabs of the 4" thick foam. Wax paper was epoxied to the bottom of one of the pieces of foam to act as the

bottom. The three slabs were stacked on top of each other with small blocks acting as spacers in between levels in order to get the mold to the required height of 15 cm. The inside edge of the ellipse was lined with wax paper and a CTDI head phantom was placed in the center of the elliptical cutout.

Immediately upon pouring the urethane mixture into the phantom mold it became apparent that the wax paper lining the inside was not strong enough to hold in the large volume of material. The wax paper bulged out at all gaps in the foam and much of the liquid rubber material spilled out. After the rubber had cured, the resulting elliptical phantom was not acceptable and the entire process was dubbed a learning experience. It was obvious that the foam and wax paper combination was not sufficient to contain the fairly viscous tissue equivalent material. It was also difficult to cut perfectly geometrical ellipses out of the thick foam by hand, and as such alternative methods were sought.

Improved Construction Methods

After the failure of the first phantom, a new method of construction was devised. Instead of the foam used previously, $\frac{3}{4}$ " plywood was purchased for use in the mold. An ellipse was cut out of three pieces of wood with the Vision Pro engraving system in the lab. The outline of the same sized ellipse was then engraved halfway through a fourth sheet of plywood that would act as the base. The Vision Pro engraving system ensured that all elliptical cutouts were uniform and of the same size. The three pieces were then stacked to a height of 15" on top of the base using wooden blocks as spacers. The interior was lined with a thick rubber sheet originally designed for lining garden ponds. Plastic molding was placed along the groove machined into the base to provide more support for the walls of the phantom mold. The CTDI head phantom was placed in the center of the mold, which was then filled with the liquid 121/30 mixture. The new setup did a

much better job of containing the liquid urethane and the phantom was left to cure overnight. Pictures of the mold and phantom building process can be found in [Figures 3-2](#) through [3-4](#).

After the urethane rubber had cured, the phantom was removed from the mold, although with some difficulty as the urethane tissue-equivalent material stuck to the wooden base layer of the mold. Other than a hard time removing the phantom, the first effort was a success and four more phantoms were constructed in a similar fashion, but with increasing major axis size while maintaining the same minor axis. The major axis lengths used in each of the five phantoms were 26cm, 28.5cm, 31.25cm, 32.6cm, and 37.25cm (+/- .25cm variation from top to bottom). The five completed phantoms are shown in [Figure 3-5](#).

Each of the five phantoms fit around a 16cm CTDI head phantom for use in CT imaging and domes measurement. The tissue equivalent material adheres to the acrylic CTDI phantom fairly well on its own, but medical tape was utilized to ensure a tight consistent fit for testing.

After construction was complete, the phantoms were used to test the functionality of the angular component of the CareDose4D[®] tube current modulation system on a Siemens Sensation 16 scanner in the Shands Orthopedic and Sports Medicine Institute at the University of Florida.

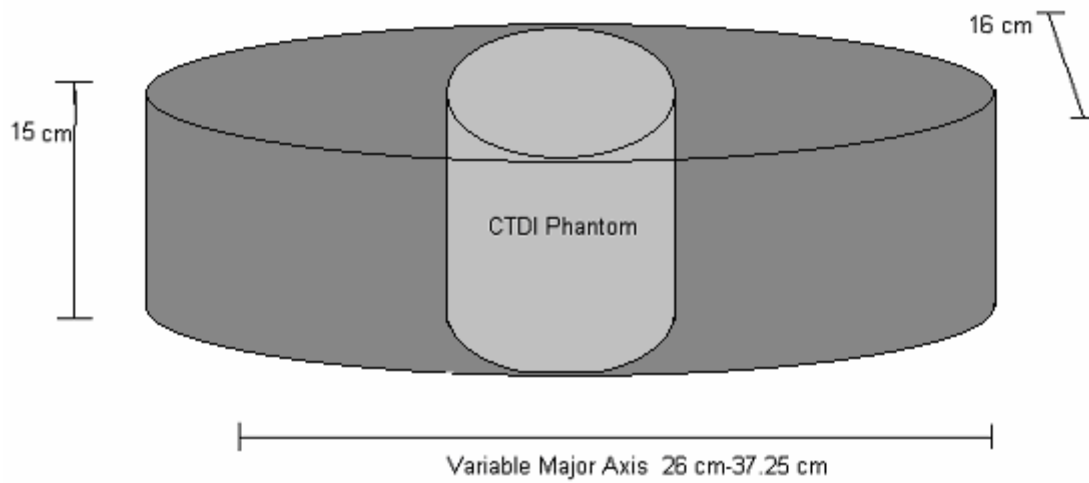


Figure 3-1: Diagram of proposed phantom design. Phantoms were designed to fit an existing CTDI phantom shown in light gray.



Figure 3-2: Elliptical phantom mold. Cutouts from other sized phantoms are visible in the plywood.



Figure 3-3: CTDI head phantom centered in phantom mold. Rubber sheeting is taped in place to contain the urethane rubber.



Figure 3-4: Phantom mold filled with urethane liquid rubber.



Figure 3-5: Five elliptical tissue equivalent phantoms of increasing major axis.

CHAPTER 4 PHANTOM TESTING

The five created elliptical phantoms were used to test the clinical functionality of the angular portion of the CareDose4D[®] tube current modulation system on a Siemens Somatom Sensation 16 CT scanner, as well as to compare doses in CT scans with fixed versus modulated tube current techniques. As previously discussed, the CareDose4D[®] system acts to modulate current along the Z-axis according to a scout scan, as well as within each tube rotation based on attenuation information from the previous 180 degrees of tube rotation. The purpose of the current modulation is to maintain a constant photon flux at the detector elements and as a result, to possibly reduce patient dose as compared to fixed current techniques. If the in-plane modulation system is working properly, image noise should remain constant for all scans at a given reference mAs setting regardless of phantom size due to the fact that image noise is related to the number of detected photons. If a larger sized phantom is being scanned, the system will compensate for the higher attenuation by increasing the tube current in order to maintain a constant number of photons at the detector, thus keeping image noise relatively constant. It should be noted that the elliptical phantoms do not test the functionality of the Z-axis modulation of the system since they are of uniform thickness along their length.

Materials and Methods

The general experimental method for the study was to measure both dose and image quality for each of the five phantoms at several reference mAs settings, and to observe trends in dose as a function of CareDose4D[®] setting and phantom size.

Phantom Dose Measurement

For all phantom measurements a standard adult abdominal routine with the same reconstruction kernel was used. The entire length of the phantom was scanned with the tube

voltage set to 120 kVp, a 5.6 second scan time, 0.5 second rotation time, 16 x 1.5mm collimation, and 18mm table feed per rotation. These parameters were held constant for all scans. The entire length of the phantom was scanned in order to allow the system to modulate the tube current. Since the angular modulation portion of the CareDose4D[®] system modulates current on the fly based on the previous 180 degrees of the scan, a single axial-slice scan, as is done for CTDI measurements, would not allow the system to properly adjust to the changes in phantom attenuation. By scanning the entire length of the phantom, which takes multiple rotations of the x-ray tube, the in-plane tube current modulation system is allowed to operate.

In order to collect dose measurements, each elliptical phantom was attached to a standard CTDI head phantom (15cm tall, 16cm diameter). The phantom was placed on the CT table and a scout image (topogram) was performed. The entirety of the phantom was selected to be scanned using six different reference mAs values (115, 130, 145, 160, 175, and 190 mAs). Each of the five elliptical phantoms was scanned at each of the previously mentioned reference mAs settings. The default setting for the adult abdominal routine is 160 mAs, and the other settings were chosen to provide a range of data points both above and below the default setting in order to check the functionality of the CareDose4D[®] system as well as to ascertain the effects of the setting on both dose and image quality in the various sized phantoms.

A Capintec (Ramsey, NJ) PC-4P pencil ion chamber was used in the center hole of the CTDI phantom to measure exposure during the scans. Exposure measurements were recorded for each scan over the entire 15cm length of the phantom. These exposure measurements were converted into integral dose measurements by multiplying each by the F-factor for soft tissue (0.94 Rad/R). This calculation is possible since the total scan length (15 cm) and table feed per rotation (1.8cm) were held constant for each phantom measurement. The integral dose, as

described by Dixon¹², is the line integral of dose measured along the Z-axis of a phantom. In the case of these measurements, the length of the scan (15 cm) was longer than the active region of the pencil ion chamber (10 cm), but this discrepancy in length was not an issue due to the width of the x-ray cone beam (approx 2.5 cm). The experimental setup for dose measurements can be seen in [Figure 4-1](#).

Phantom Image Quality Measurement

In order to measure image quality as a function of reference mAs setting and phantom size, the uniformity portion of a Catphan 440 (The Phantom Laboratory, Salem NY) image quality phantom was used. Scans were performed at each of the previously mentioned reference mAs settings with each of the five elliptical phantoms. Minimum and maximum CT number values were measured in five regions of interest- each 4 cm in diameter- in the reconstructed image, as shown in [Figure 4-2](#). The values from each of these five regions were averaged together to provide the average minimum and maximum CT numbers for the uniformity region of the Catphan. Based on these average maximum and minimum CT number values, the image uniformity for each h scan was calculated using Equation 4-1.

$$Image\ Uniformity = [1 - ((max - min) / (max + min))] \quad (Eq. 4-1)$$

A uniformity value of one indicates that the region is completely uniform, while lower uniformity values indicate a greater degree of variation in CT number values as a result of image noise.

The uniformity portion of the Catphan 440 was used for image quality measurements instead of the CTDI head phantom used for dose measurements because it provided an entirely uniform volume for measurement. The CTDI phantom has five drilled out segments (one in the

center, and four around the periphery) for pencil ion chamber placement. While these drilled out portions are filled with acrylic rods when not in use for dose measurements, there was concern that the small air gaps around each rod could alter the minimum and maximum CT number values in the reconstructed image and provide a source for variation and error in the results.

Comparison of Modulated and Fixed Tube Current Techniques

Tests were also performed in order to determine the differences in dose and image quality between tube current modulated scans and those performed with fixed-current techniques. For purposed of clarity and simplicity, only three elliptical phantoms (with major axes of 26, 31.25, and 37.25 cm) were used in these experiments. Each phantom was scanned with the CareDose system at reference mAs settings of 100, 150, and 200 mAs. The phantoms were then scanned with a fixed tube current technique with effective mAs settings of 100, 150, and 200 mAs. Dose for each scan was measured in the same manner previously described. In the interest of time, CT number standard deviation was used in place of uniformity as a measure of image quality. A lower CT number deviation indicates a more uniform reconstructed image. All other scan parameters were the same as previously described under the dose and image quality sections.

Results and Discussion

The image uniformity and dose measurements for each phantom at each of the six reference mAs values were plotted in order to verify proper in-plane CareDose4D[®] function, as well as to observe trends in dose and image quality as a function of reference mAs setting and phantom size.

Image Uniformity Measurements

The effects of phantom major axis length and reference mAs setting on image uniformity are illustrated in [Figure 4-3](#). As expected, image uniformity remains constant (within bounds of experimental error) for each reference mAs setting, regardless of phantom axis length. Error bars

were not included in [Figure 4-3](#) for purposes of clarity, but image uniformity for each reference mAs setting with associated error bars can be found in Appendix A. Image uniformity is also seen to increase as the reference mAs setting was increased. As expected, each increase in the reference mAs setting yields an increase in the image uniformity, indicating a decrease in image noise. This is a result of the tube current modulation system increasing the photon output of the x-ray tube in order to attempt to match the total effective mAs of the scan to that of the reference setting.

An interesting trend is observable in [Figure 4-3](#) in which image uniformity for phantoms 2 through 4 is slightly lower than for phantoms 1 and 5. This trend is seen across all reference mAs settings, although the uniformity values for phantom 4 migrate towards that of phantom 5 starting at a reference mAs setting of 160. While all uniformity values were found to be within bounds of experimental error, the repeating trend for all measurements is worth notice, and can be attributed to one of two sources. The first and most probable source for this trend is the reconstruction algorithm itself. While no changes were made to the reconstruction kernel used for each scan, the system itself makes adjustments in its reconstruction method in order to produce the reconstructed image. It is possible that such changes took place for the three midsized phantoms in this testing. A second possible source of the trend could be attributable to systematic human error during the testing. Although every step was made to use the same procedure and techniques when performing each scan, it is not outside the realm of possibility that some such changes, such as exact phantom placement on the CT table, were made. A repeat of all tests would be required to determine if the trend is reproducible, which would suggest its roots were in the reconstruction algorithm.

The percentage increase in uniformity for each increase in reference mAs (referenced to the 115 reference mAs setting) can be seen in [Figure 4-4](#). Again, error bars are not included for purposes of clarity. Although it appears that a trend towards larger increases in uniformity for larger phantom sizes exists, when the data is plotted with error bars (shown in [Figure 4-5](#) for only the 190 reference mAs setting) it is apparent that all points are well within bounds of experimental error and no such trend can be inferred.

Dose Measurements

The effects of phantom major axis and reference mAs setting on integral dose are shown in [Figure 4-6](#). As expected, dose increased as the phantom major axis increased for each given reference mAs setting. This is attributable to the CareDose4D[®] system increasing the tube current in response to the added attenuating material in order to maintain a constant photon flux at the detector elements. The larger phantoms attenuate more of the incoming beam and thus require larger tube currents in order to maintain the same image quality. These larger tube currents in turn cause a higher dose in the phantom.

Integral dose measurements were also found to increase as the reference mAs setting was increased. The increase as a result of changing reference mAs setting was fairly uniform for each phantom size as is seen by the even spacing between each reference mAs setting line in [Figure 4-6](#) across all phantom sizes. This increase in integral dose averaged an increase of 13% (+/- 0.75) per increase of 15 in the reference mAs setting for all sized phantoms.

A noticeable trend found in [Figure 4-6](#) is the larger integral dose values for the largest phantom (phantom 5) as compared to those of the other phantoms within each reference mAs grouping. This is most likely attributable to non uniform spacing of the phantom's major axes. The phantoms major axes measure 26 cm, 28.5 cm, 31.25cm, 31.6 cm and 37 cm respectively, with approximately 2 cm gaps between each of the first four phantoms, and a relatively larger

(~5 cm) gap between phantoms 4 and 5. This larger gap equates to a phantom with a larger amount of attenuating material which could explain the jump in dose to phantom 5 as the modulation system attempts to maintain a constant photon flux at the detector.

Overall Trends

The average increase in integral dose from one reference mAs setting to the next was found to be fairly constant at 13% (+/- 0.75%). The average increase in image uniformity for each increase of 15 in the reference mAs setting was found to be 2.5% (+/- 0.79%). Both of these measurements were found to increase linearly across the range of reference mAs values utilized. It is hypothesized that if the reference mAs setting were increased further, dose measurements would continue to rise, but gains in image uniformity would fall off as the limits of the scanner's detectors were reached.

Comparison of Modulated and Fixed Tube Current Techniques

The results of the comparison study between modulated and fixed tube current techniques are shown in [Figures 4-7](#) and [4-8](#). In comparing the image quality between the two modes of acquisition, several trends are visible. As expected, pixel deviation in the reconstructed images is seen to decrease as the tube current is increased for both fixed and modulated techniques. This is expected as the higher number of photons reaching the detector at higher tube currents reduces the effects of random image noise. The pixel deviation for the tube current modulated techniques is seen to remain fairly constant regardless of phantom size. As previously mentioned, this indicates that the in-plane tube current modulation system was properly working to maintain a constant photon flux at the detector. In the fixed tube current scans, pixel deviation is seen to increase with phantom size. This is also as expected since the larger phantoms attenuated more of the fixed photon output, a situation that results in fewer photons reaching the detector for larger phantom sizes. Fewer photons reaching the detector cause an increase in image noise, and

as such, an increase in the standard deviation of pixel values in a uniform area. These results demonstrate the need for features such as tube current modulation, since image noise in a patient scan can vary from slice to slice depending on anatomy with fixed current techniques. Systems such as CareDose act to maintain a constant image noise throughout an entire scan.

The effects of dose in the comparison study are seen in [Figure 4-8](#). As a general trend, doses were seen to increase as tube current setting was increased for both modulated and fixed technique scans. As seen previously, the dose from the tube current modulated scans was seen to increase slightly as phantom size increased. This was a result of a larger x-ray tube output in order to compensate for more attenuation in the phantom in order to maintain a constant flux at the detector. Conversely, doses were seen to decrease as phantom size increased in the fixed current scans. This again is explained by the higher photon attenuation in the larger phantoms. Unlike in the modulated technique scans, the fixed current technique does not adjust for the increase in attenuation in larger phantoms and as such, the dose in the center of the phantom is lower, but at the expense of noisier images.

In comparing the doses between the two techniques, the tube current modulated techniques all produced lower doses than fixed tube techniques. The magnitude of the dose savings increased with phantom size, and ranged from 49% for the smallest phantom to 62% for the largest phantom size. These percentage dose savings were constant for each mAs setting. That is, regardless of mAs setting, the dose reduction by switching to the tube current modulated scan versus the fixed current technique was the same for each phantom size.

These decreases in dose came at the expense of slightly noisier images in the tube current modulated scans. As seen in [Figure 4-7](#) the pixel deviation was found to be higher in the tube current modulated scans as compared to the fixed technique scans at similar settings. These

differences again were found to be based on phantom size, and ranged from 64% to 90% lower pixel deviations in the fixed tube current scans for the small to large phantoms respectively.

Conclusions

A compressible tissue equivalent material was developed and successfully used to build five elliptical phantoms of varying major axis length. These phantoms were then used to show the proper functionality of the angular portion of the Siemens CareDose4D[®] tube current modulation system in a Somatom Sensation 16 CT scanner. The image uniformity values in reconstructed images from each phantom were found to be the same, within bounds of experimental error, at each of six tested reference mAs values for an adult abdominal routine, indicating that the modulation system was properly adjusting the tube current in response to the amount of attenuating material in the beam. This method could easily be worked into a regular monthly or quarterly quality assurance plan for the CT scanner in order to ensure proper operation of the tube current modulation system. Individual scanner performance could be tracked over its useful life and action limits could be set if uniformity values begin to drift.

In addition to quality assurance, general trends in image quality and dose were observed as a function of variation in reference mAs setting and phantom major axis. An increase in integral dose of 13% was found for each increase of 15 in the reference mAs setting, while image uniformity increased by approximately 2.5% for each such increase. Knowledge of such trends could help aid radiologists and technologists in selected a proper CareDose4D[®] reference mAs setting for a given exam in order to minimize patient doses while maintaining clinically acceptable image quality.

In comparing the modulated to fixed tube current techniques, it was shown that dose reductions of over 50% were possible by using an in-plane modulation system. These reductions did come at the cost of increased image noise, and further tests would be required in order to

determine an acceptable level of image noise in diagnostic images. It is possible that the increase in image noise as a result of these dose reductions would not affect the diagnostic acceptability of the images.



Figure 4-1: Experimental setup for dose measurements. A pencil ion chamber is placed in the center of a CTDI head phantom with a tissue equivalent elliptical phantom during a CT scan.



Figure 4-2: Screen capture of a CT scan of an elliptical phantom surrounding a uniform region of an image quality phantom. The five regions of interest used for measuring CT # uniformity values are shown as black circles in the center phantom.

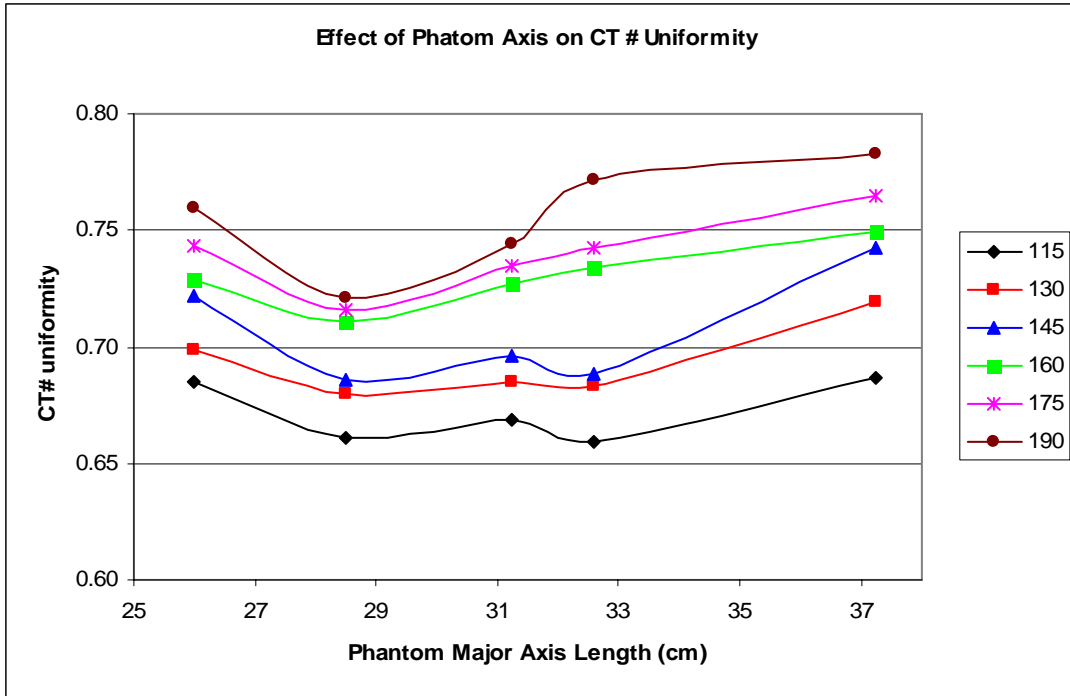


Figure 4-3: CT number uniformity as a function of phantom major axis and reference mAs setting

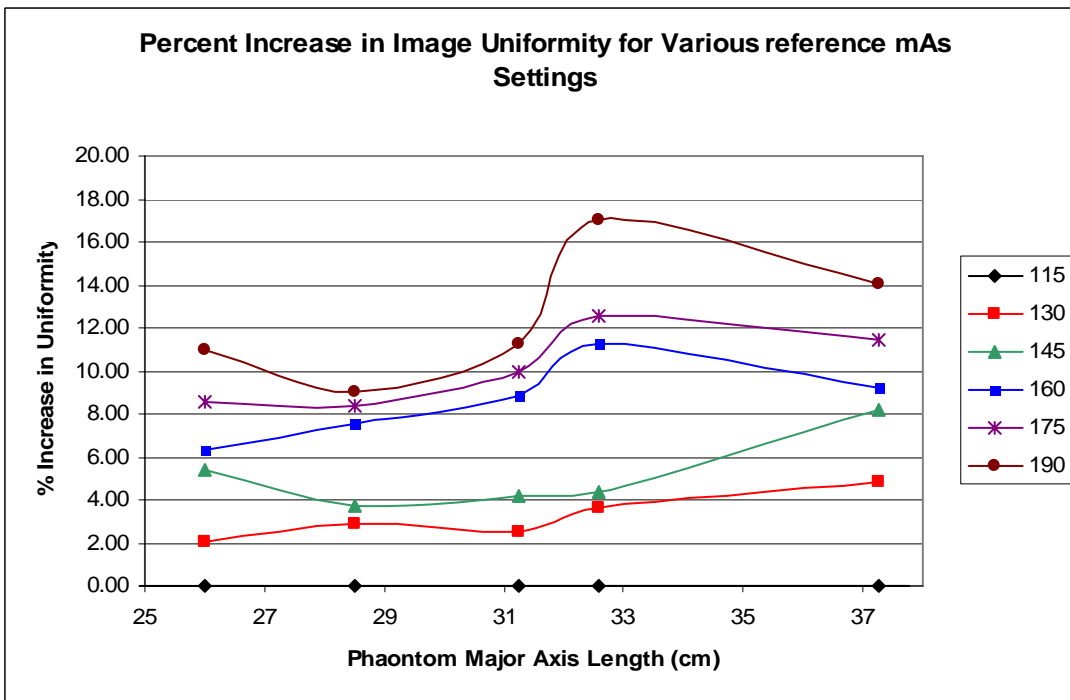


Figure 4-4: Percent increase in CT number uniformity for increasing reference mAs settings

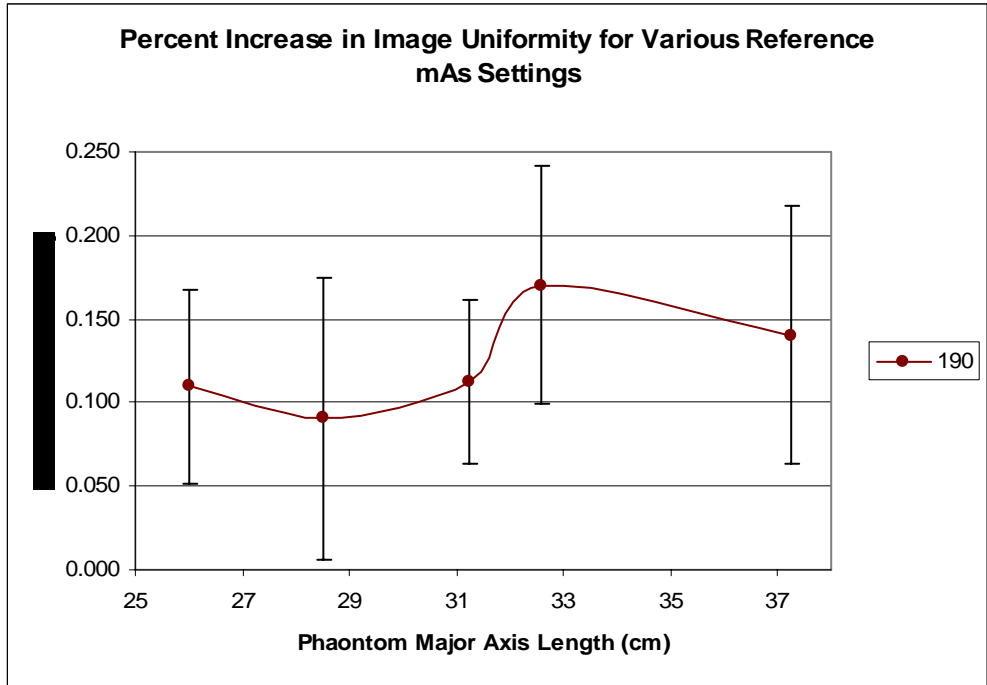


Figure 4-5: Percent increase in CT uniformity with error bars for 190 reference mAs setting

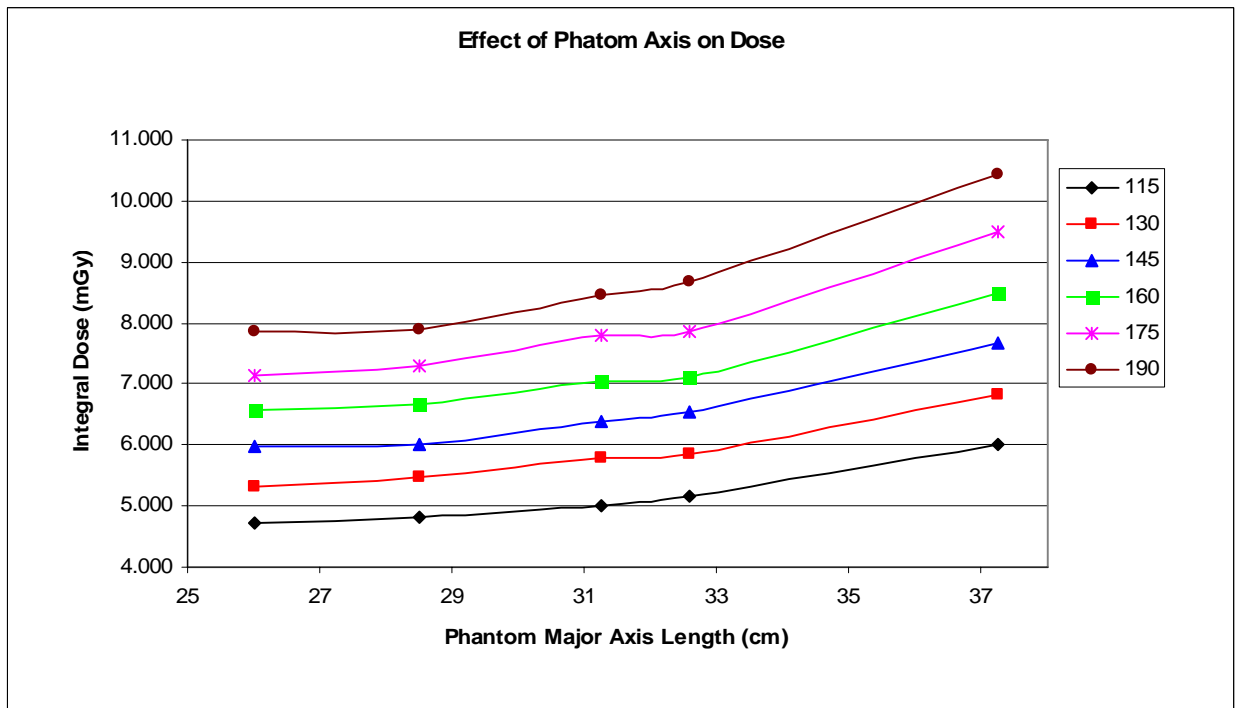


Figure 4-6: Increases in dose as a result of changes in phantom major axis length and reference mAs setting.

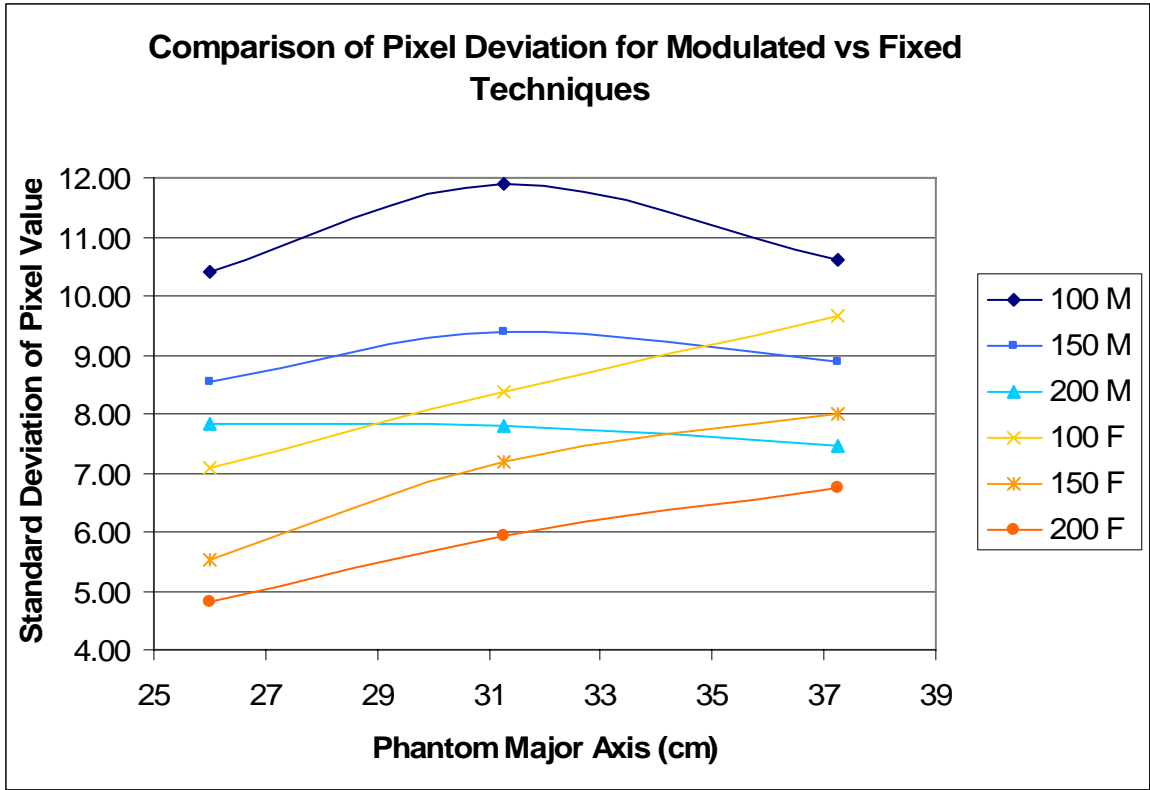


Figure 4-7: Comparison of image quality between modulated and fixed tube current techniques. In the legend, M indicates tube current modulation, and F indicates fixed tube current techniques.

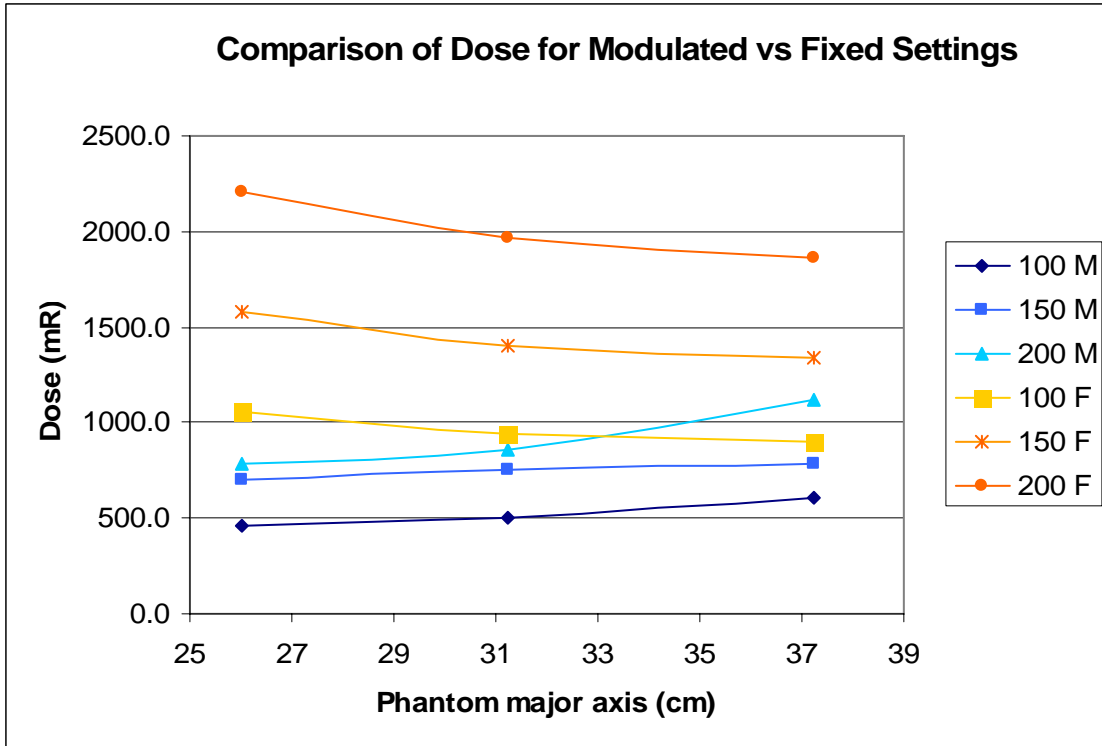


Figure 4-8: Comparison of dose between modulated and fixed tube current techniques. In the legend, M indicates tube current modulation, and F indicates fixed tube current techniques.

CHAPTER 5 FUTURE WORK

Future work is planned in further characterizing the tissue equivalent material developed. The characterization of attenuation properties will be expanded to ensure that the material is equivalent to human soft tissues at a wider range of beam energies. The radiological properties of the tissue equivalent material will also be documented in more detail, paralleling the work of Kyle Jones, a recent doctoral graduate of the program who developed the epoxy based tissue equivalent materials previously in use in the lab.

There are also several outlets for future work utilizing the phantoms and methods described in this thesis. The tissue equivalent material is already being utilized in another project to create a tomographic adult CT phantom. Such a phantom would serve to provide specific organ dose measurements from CT scans which could be correlated to Monte Carlo simulations using the data the phantom was created from.

The Smooth-On PMC 121/30 urethane rubber utilized to make a soft tissue equivalent material is also being used as a base for the development of a breast tissue equivalent material. Recipes for materials equivalent to breast tissues of varying composition and ratios of glandular to fatty tissue are in development. It is hoped that such materials can be used in the construction of more realistic mammographic phantoms than those currently in widespread use. Such anatomical phantoms could be used to better characterize equipment and patient doses associated with mammography.

The five created phantoms could also be used to further characterize dose and image quality in next generation 32 and 64 slice CT scanners. Characterization of dose and image quality as a function of tube current modulation setting and patient size is of paramount importance as wider beams and more slices can drastically increase patient doses. The same

benefits of this current work would thus be extended to these newer scanners. Plans are also in place to develop phantoms to test Z-axis tube current modulation specifically. Such phantoms would need to change dimensions along the Z-axis of a CT scan, something the current phantoms do not accomplish.

The phantoms would also be extremely useful in comparing the dose savings and gains in image quality across CT scanners from different manufacturers. Currently some form of tube current modulation is in place in most commercially available CT scanners, but the methodology utilized by companies can vary greatly. Often the specifics of the algorithms used by the companies are not fully disclosed due to their proprietary nature. The created phantoms could be used to qualitatively compare the functionality of these varied.

The created phantoms could also be used to characterize location dependant image quality in phantoms. It was qualitatively observed during the course of this research that image noise was higher towards the center of the phantoms as compared to around the periphery. Further studies could clarify and quantify these differences in image quality, and their dependence on tube current modulation setting and phantom size. This information would obviously be helpful to radiologists in knowing the degree to which image noise changes throughout an image.

Lastly, plans for position dependant dose measurements within the phantoms are being developed along with a fiber optic dosimetry system.

APPENDIX
IMAGE UNIFORMITY GRAPHS

The following are the graphs of image uniformity as a function of phantom major axis for each of the individual reference mAs settings. Error bars are included to show that uniformity remains constant within bounds of experimental error regardless of phantom size.

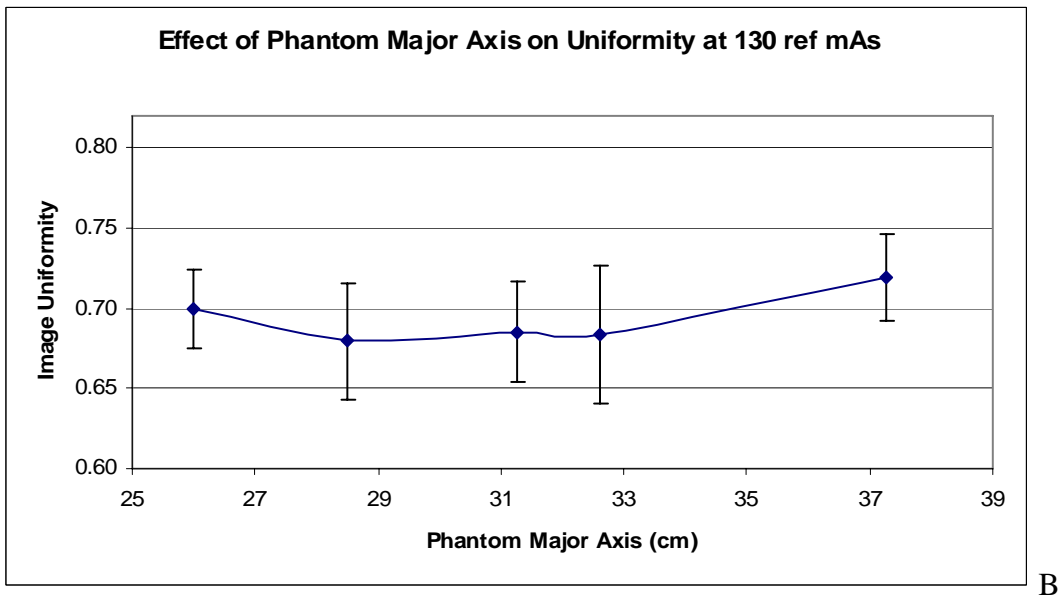
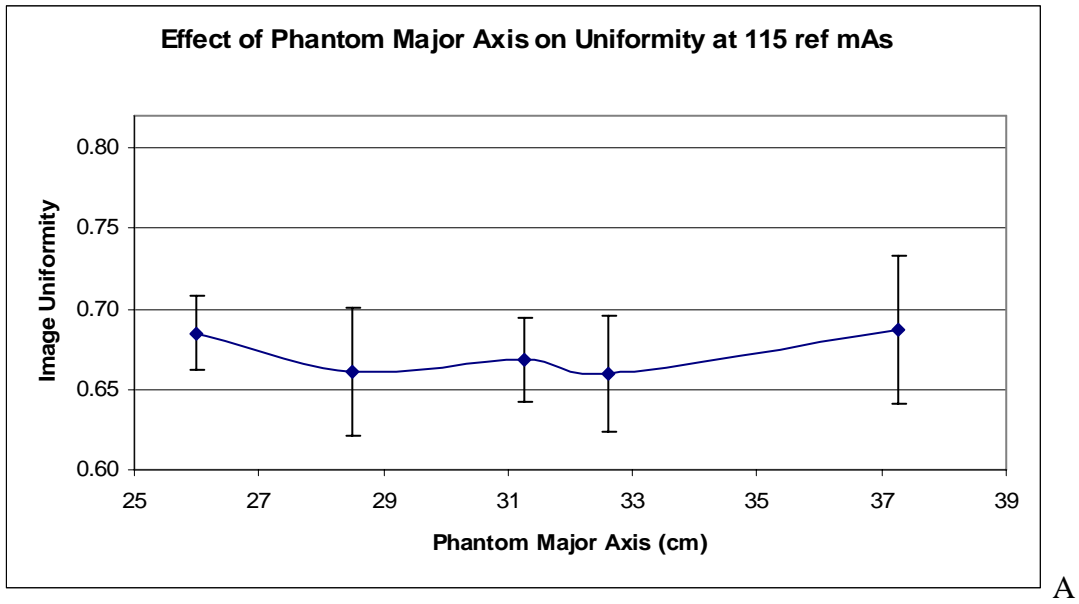
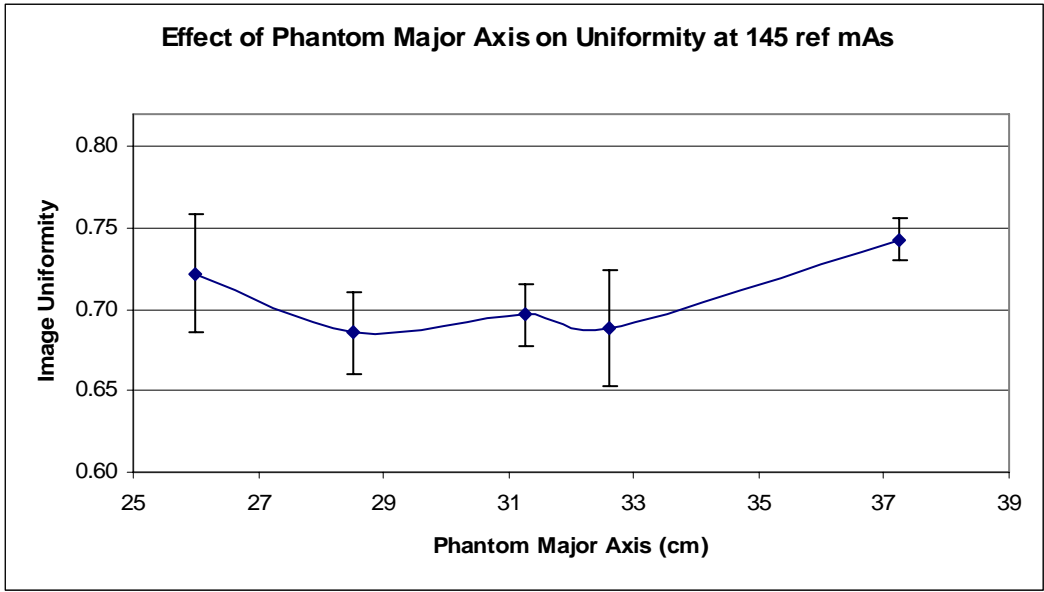
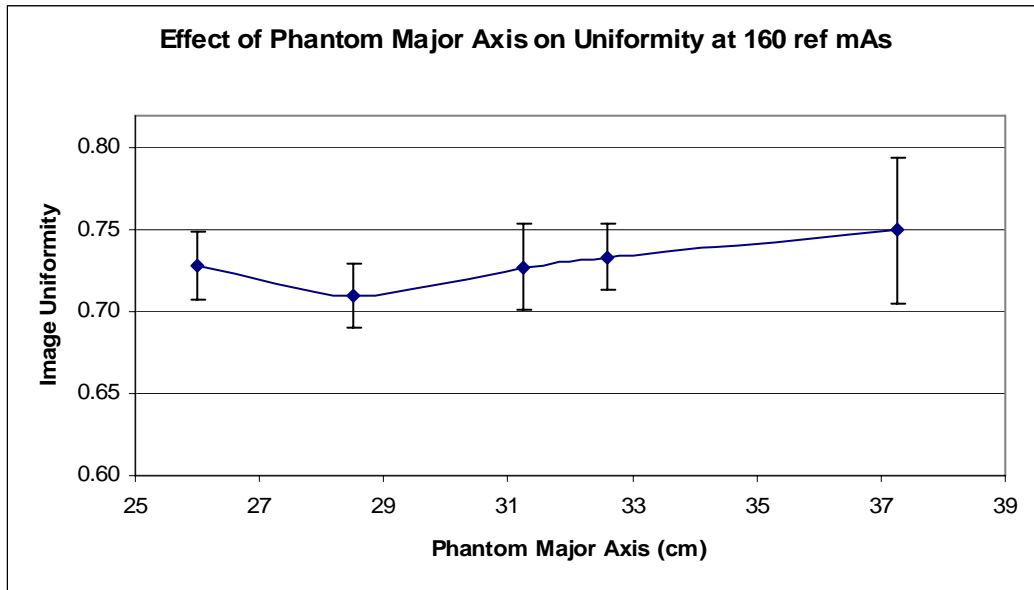


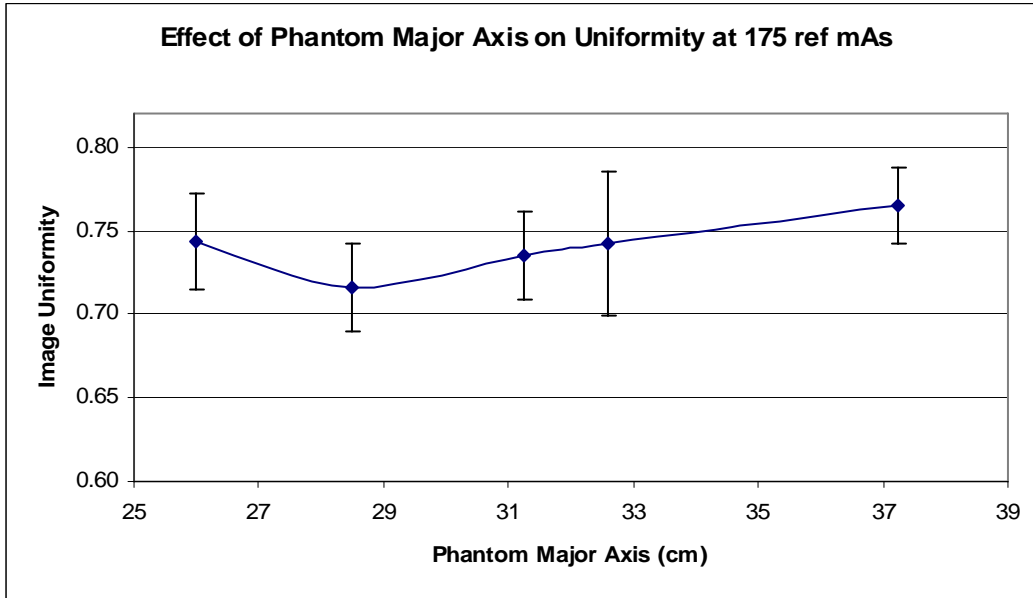
Figure A-1: CT number uniformity as a function of phantom major axis for a reference mAs setting of A) 115, B) 130, C) 145, D) 160, E) 175, F) 190.



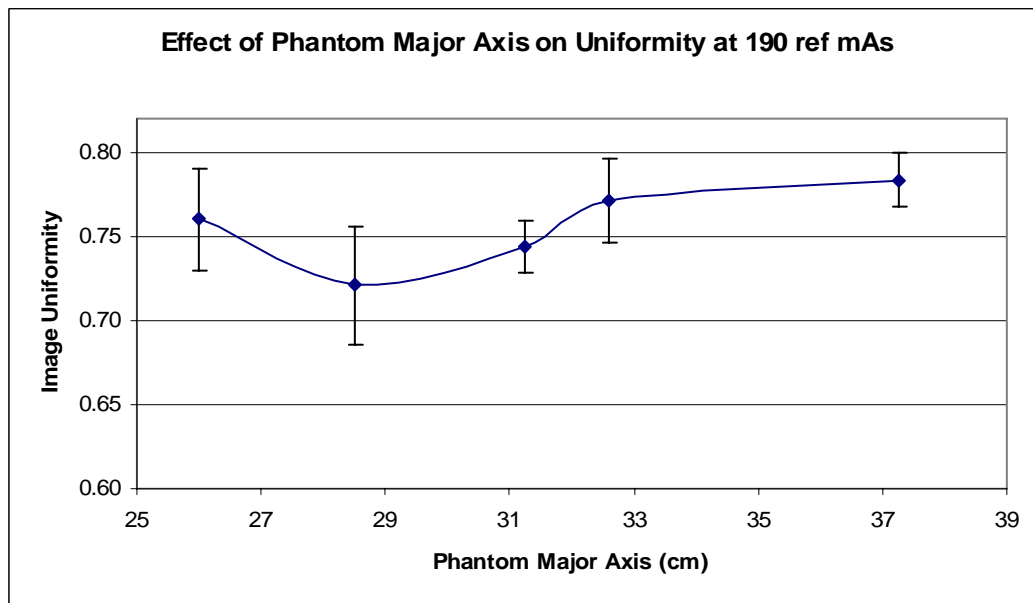
C



D



E



F

LIST OF REFERENCES

- ¹ M. Kalra, M. Maher, T. Toth, L. Hamberg, M. Blake, J. Shepard, and S. Saini, "Strategies for CT Radiation Dose Optimization," *Radiology* **230**, 619-628 (2004).
- ² H. Grees, J. Lutze, H. Wolf, T. Hothorn, and W. Bautz, "Dose Reduction in Subsecond Multislice Spiral CT Examination of Children by Online Tube Current Modulation," *Eur. Radiol.* **14**, 995-999 (2004).
- ³ M. Kalra, M. aher, T. Toth, B. Schmidt, B. Westerman, H. Morgan, and S. Saini, "Techniques and Applications of Automatic Tube Current Modulation for CT," *Radiology* **233**, 649-657 (2004).
- ⁴ M. Geis, W. Kalender, H. Wolf, and C. Suess, "Dose Reduction in CT by Anatomically Adapted Tube Current Modulation I Simulation Studies," *Med. Phys* **26**, 2235-2247 (1999).
- ⁵ J. Althen, "Automatic Tube Current Modulation in CT- A Comparison between Different Solutions," *Radiation Protection Dosimetry* **114**, 308-312 (2005).
- ⁶ W. Kalender, H. Wolf, and C. Suess, "Dose Reduction in CT by Anatomically Adapted Tube Current Modulation II Phantom Measurements," *Med. Phys* **26**, 2248-2253 (1999).
- ⁷ M. Kalra, M. Maher, T. Toth, R. Kamath, E. Halpern, and S. Saini, "Comparison of Z-Axis Automatic Tube Current Modulation Technique with Fixed Tube Current CT Scanning of Abdomen and Pelvis," *Radiology* **232**, 347-353 (2004).
- ⁸ M. Kalra, M. Maher, R. D'Souza, S. Rizzo, E. Halpern, M. Blake, and S. Saini, "Detection of Urinary Tract Stones at Low-Radiation-Dose CT with Z-Axis Automatic Tube Current Modulation: Phantom and Clinical Studies," *Radiology* **235**, 523-529 (2005).
- ⁹ M. Kalra, S. Rizzo, M. Maher, E. Halpern, T. Toth, J. Shepard, and S. Aquino, "Chest CT Performed with Z-Axis Modulation: Scanning Protocol and Radiation Dose," *Radiology* **237**, 303-308 (2005).
- ¹⁰ S. Rizzo, M. Kalra, B. Schmidt, T. Dalal, C. Suess, T. Flohr, M. Blake, and S. Saini, "Comparison of Angular and Combined Automatic Tube Current Modulation Techniques with Constant Tube Current CT of the Abdomen and Pelvis," *Am J Roentgenol* **186**, 673-679 (2006).
- ¹¹ C. Suess, and X. Chen, "Dose Optimization in Pediatric CT: current technology and future innovations," *Pediatr. Radiol* **32**, 729-734 (2002).
- ¹² R. Dixon "Restructuring CT dosimetry- A realistic strategy for the future Requiem for the pencil chamber," *MedPhys* **33** (10), 3973-3976 (2006).

BIOGRAPHICAL SKETCH

Ryan Fisher graduated from Brookwood High School in 2000. Brookwood is located in Snellville Georgia, a suburban town 25 miles northeast of Atlanta. Ryan then attended The Georgia Institute of Technology (Georgia Tech) and graduated with a Bachelor of Science degree in biomedical engineering in 2004. He then enrolled at the University of Florida to pursue master's and doctorate degrees in medical physics.